UPPSALA
UNIVERSITET

Digital Comprehensive Summaries of Uppsala Dissertations from the Faculty of Science and Technology 820

Numerical Simulations of Long Spark and Lightning Attachment

LILIANA AREVALO

ACTA
UNIVERSITATIS
UPSALIENSIS
UPPSALA
2011

ISSN 1651-6214
ISBN 978-91-554-8060-8
urn:nbn:se:uu:diva-149171

Dissertation presented at Uppsala University to be publicly examined in Häggsalen, Ångström Laboratory, Lägerhyddsvägen 1, Uppsala, Wednesday, May 25, 2011 at 10:00 for the degree of Doctor of Philosophy. The examination will be conducted in English.

Abstract
Arevalo, L. 2011. Numerical Simulations of Long Spark and Lightning Attachment. Acta Universitatis Upsaliensis. *Digital Comprehensive Summaries of Uppsala Dissertations from the Faculty of Science and Technology* 820. 91 pp. Uppsala. ISBN 978-91-554-8060-8.

The research work presented here is concerned with numerical simulations of two different electrical phenomena: Long gap electrical discharges under switching impulses and the lightning attachment process associated with positive upward leaders. The development of positive upward leaders and the progression of discharges in long gaps are attributable to two intertwined physical phenomena, namely, the leader channel and the streamer zone. The physical description and the proposed calculations of the above-mentioned phenomena are based on experimental tests conducted in long spark gaps.

The methodology presented here proposes a new geometrical approximation for the representation of the streamer and the calculation of the accumulated electrical charge. Furthermore, two different approaches to representing the leader channel are applied and compared. Statistical delays before the inception of the first corona, and random distributions to represent the tortuous nature of the path taken by the leader channel were included based on the behavior observed in experimental tests, with the intention of ensuring the discharge behaved in a realistic manner. A reasonable agreement was found between the physical model and the experimental test results.

A model is proposed to simulate the negative discharges produced by switching impulses using the methodology developed to simulate positive leader discharges and the physics underlying the negative leader phenomena. The validation of the method demonstrated that phenomena such as the pilot leader and negative leader currents are successfully represented.

In addition, based on previous work conducted on the physics of lightning and the lightning attachment process, a new methodology is developed and tested. In this new approach, the background electric field and the ionized region, considered in conjunction with the advance of the leader segment, are computed using a novel method. The proposed methodology was employed to test two engineering methods that are accepted in international standards, the mesh method and the electro-geometrical method. The results demonstrated that the engineering approximations are consistent with the physical approach.

In addition to the electrical phenomena mentioned above, one should remember that, to simplify the calculation, there are certain real effects arising from the lightning attachment process that have not been considered. In fact, when a structure is subjected to a strong electric field, it is possible to generate multiple upward leaders from that structure. This effect has not been taken into account in the numerical models available previously, and therefore the process of generating multiple upward leaders incepted over a structure is incorporated here. The results have shown that a slight advantage from the background electric field is enough for one upward connecting leader to take over, thereby forcing the others to abort the attachment process.

Keywords: breakdown, discharge, leader channel, lightning attachment, negative discharge, positive discharge, streamer

Liliana Arevalo, Faculty of Science and Technology, Box 256, Uppsala University, SE-75105 Uppsala, Sweden.

ISSN 1651-6214
ISBN 978-91-554-8060-8
urn:nbn:se:uu:diva-149171 (http://urn.kb.se/resolve?urn=urn:nbn:se:uu:diva-149171)

To my grandparents: Mujita and "el papito" Telésforo for giving me all the love and courage that have helped me to face each stage of my life" ... I know you would be proud of this

and

Teo, Clarita, Myriamcito,
Mami, Guillo, Marthica and Vivis
Thanks for teaching me how to pursue my dreams and giving me the strength to always continue

List of Papers

This thesis is based on the following papers, which are referred to in the text by the Roman numerals assigned below.

I **Arevalo L**, Cooray V, Montaño R, and Roman F: "Modeling of positive discharges in laboratory gaps under switching impulses". Paper presented at the *XVII International Conference on Gas Discharges and their Applications GD2008*; September, 2008.

II **Arevalo L,** Cooray V, and Montaño R: "Breakdown effect in long gaps under switching impulses: statistical variation". Paper presented at the *29th International Conference on Lightning Protection ICLP 2008*; June, 2008.

III **Arevalo L**, Cooray V, and Montaño R: "Breakdown times and voltages probability calculation using a simplified numerical methodology". Paper presented at the *35th Grounding and 3rd Lightning Physics Conference — GND & LPE*; November, 2008.

IV **Arevalo L**, Cooray V, and Montaño R: "Numerical simulation of long sparks generated by positive switching impulses." Published paper *Journal of Electrostatics* Vol 67/2 - 3 (2009) ISSN 0304-3886 pp. 228 - 234.

V **Arevalo L**, Cooray V, and Wu D: "Laboratory long gaps simulation considering a variable corona region". Paper presented at the *30th International Conference on Lightning Protection ICLP 2010*; September, 2010.

VI **Arevalo L**, Cooray V, and Wu D: "A reliable numerical method for the calculation of breakdown voltages". Paper presented at the *30th International Conference on Lightning Protection ICLP 2010* - September, 2010.

VII **Arevalo L**, Cooray V, Wu D and Jacobson B: "A new static calculation of the streamer region for long spark gaps". Paper submitted to *Journal of Electrostatics*

VIII **Arevalo L**, Cooray V, Wu D and Jacobson B: "The development of long spark gaps: Simulation including a variable streamer region". Paper submitted to *IEEE Transactions on Dielectrics and Insulation Materials.*

IX **Arevalo L**, and Cooray V: "Reliable model for the calculation of negative leader discharges under switching impulses". Paper presented at the *36th Grounding and 4th Lightning Physics Conference - GND & LPE*; November, 2010.

X **Arevalo L**, and Cooray V: "A preliminary model to simulate negative leader discharges". Paper submitted to *Journal of Applied Physics D*

XI **Arevalo L**, and Cooray V: "On the interception of lightning flashes by power transmission lines". Accepted for publication by *Journal of Electrostatics*.

A resume paper of this manuscript was presented at the *Nordic Insulation Symposium NORD – ISS*; June, 2009.

XII **Arevalo L,** and Cooray V. "The mesh method in lightning protection Standards — Revisited" *Journal of Electrostatics* Vol 68 Issue 4, August, 2010, pp. 311 - 314.

A resume paper of this manuscript was presented at 30th International Conference on Lightning Protection ICLP 2010- September, 2010

XIII **Arevalo L,** and Cooray V: "Influence of multiple upward connecting leaders initiated from the same structure on the lightning attachment process." Paper presented at the *International Symposium on Lightning Protection - SIPDA X*; November, 2009.

XIV Cooray V, Fernando M, **Arevalo L**, and Becerra M: "Interaction of multiple connecting leaders issued from a grounded structure simulated using a self consistent leader inception and propagation model". Paper presented at *30th International Conference on Lightning Protection ICLP 2010*; September, 2010.

The author has contributed to other publications which are not incorporated in this thesis, these are as follows:

XV Cooray V, **Arevalo L**, Rahman M, Dwyer J, and Rassoul H. "On the possible origin of X-rays in long laboratory sparks". *Journal of Atmospheric and Solar Terrestrial Physics.* Vol 71 Issues 17 – 18. pp. 1890 – 1898. December, 2009.

XVI **Arevalo L**, Diaz O., and Mejia A. "Design and construction of Surge Protection Devices for rural distribution transformers based on the hygroscopic properties of sand". *International Symposium on Lightning Protection – SIPDA IX.* Brazil 2007.

XVII O Diaz, **Arevalo L**, and Roman F. "Understanding the corona space charge influence on the ESD-like discharge produced by a floating electrode in a fast impulse current generator". *International Symposium on Lightning Protection – SIPDA IX*. Brazil, 2007.

XVIII O Diaz, **Arevalo L**, Cooray V, and Mejia A: "Electrical breakdown in soil under uniform background electric fields". Paper presented at the *36th Grounding and 4th Lightning Physics Conference - GND & LPE*; November, 2010.

Reprints were made with permission from the respective publishers.

The Scientific Committee of the
International Conference on Lightning Protection
(ICLP) presents the

Young Scientist Award

presented to

Liliana Arevalo

who has delivered an oral or poster presentation of high quality entitled

"...Three oral presentations and two posters....."

at the International Conference on Lightning Protection and has made notable contributions in the field of lightning research and lightning protection

30th International Conference on Lightning Protection
ICLP 2010
Cagliari, ITALY
13 - 17 September 2010

István Berta
Chairman of the Awards Committee

Farhad Rachidi
President

Carlo Mazzetti and Carlo Alberto Nucci
30th ICLP Co-Chairpersons

European Working Party
„Static Electricity in Industry"
(EFCE)

Young Scientist Award

has been given to

LILIANA PATRICIA AREVALO GEL

who has delivered a presentation of high quality
at the International Conference on Electrostatics and
has made notable contributions in the field of industrial
electrostatics

Presented at the

11th International Conference
on
Electrostatics
Valencia, Spain
27 - 29 May 2009

M. Glor
Chairman of the Working Party

Secretary of the Working Party

Conference Chairman

Scientific Committee
of the
International Conference on Lightning Protection
(ICLP)

DIPLOMA

to

Liliana Arevalo

who has delivered a presentation of high quality at the
International Conference on Lightning Protection
entitled " Breakdown Effect on Long Gaps Under Switching Impulses Statistical Variation "
and has made notable contributions to the field of lightning research and lightning protection

29th International Conference on Lightning Protection
ICLP 2008
Uppsala, Sweden
23 - 26 June 2008

.....
President of the Scientific Committee
Carlo Mazzetti

.....
Chairman of the Award Committee
István Berta

.....
Vice-President and Conference Chairman
Vernon Cooray

Contents

1 Introduction 21

2 The behavior of positive switching impulses in long spark gaps 24
2.1 The mechanism underlying positive leader discharges 25
2.2 Leader inception models 27

3 A simplified and a complete methodology to calculate the breakdown process in long spark gaps under positive switching impulses 31
3.1 Simplified methodology for the simulation of long spark gaps 31
3.1.1 The initial methodology 31
3.1.2 The statistical variations 33
3.1.3 Comparison of the equations for two different leaders 36
3.2 Full version of the long spark calculation for a variable streamer region 40
3.2.1 Methodology 41
3.2.2 Results of the simulations 46

4 Validation of the methodology through ultra high voltage laboratory experiments 50
4.1 Experimental set-up 50
4.1.1 Rod-plane air gaps 51
4.1.2 Sphere-plane configuration 53
4.1.3 Variable distance to the wall 54

5 Negative leader discharges under switching impulses 57
5.1 Mechanism behind negative leader discharges 57
5.2 Negative leader models 58
5.3 A preliminary model to simulate negative leader discharges under switching impulses 59
5.3.1 “Pilot streamer system” 61
5.3.2 “Negative leader phase” 62
5.4 Application of the methodology 63

6 The lightning attachment process and applications to IEC standards 66
6.1 Lightning protection models and standards 66
6.2 Lightning attachment model 67
6.2.1 The methodology 68
6.2.2 Applications to the lightning attachment process 70
6.3 Multiple connecting leaders from a grounded structure 75

7 Conclusions....78
8 Future Work....81
Svensk sammanfattning....83
Acknowledgements....85
References....87

Nomenclature

A		A constant that depends on the electrode configuration in Rizk model (equation 2.1)
A, b		Constants required to calculate the final jump distance (equation 5.1)
a_i	[m]	The distance between the streamers from Goelian and Lalande's model
a_i	[m]	The radius of the leader segment i at a set time in Gallimberti's leader model (equation 3.11)
a_{0i}	[m]	The initial radii of the leader for Gallimberti's leader model equation
dt	[s]	An infinitesimal time interval
dl	[m]	The length of each segment of the leader channel
E_i	[V/m]	The electric field at the start of the leader
E_{sc}	[V/m]	The electric field in the streamer zone
E_∞	[V/m]	The potential gradient of the fully developed leader channel
E_{Li}	[V/m]	The potential gradient across the leader at segment i
H	[m]	The height of the grounded structure under consideration of the electro-geometrical method. (equation 5.4)
H	[m]	The height of the cloud (assumed to be equal to 4000 m) for Cooray et al's downward leader (equation 5.3)
h_f	[m]	The height of the conductor using the protection cone method
h_g	[m]	The height of the shielding wire using the protective cone method
I_p	[kA]	The peak magnitude of the prospective lightning current

I_L	[A]	The current injected into the leader channel
K		A geometric constant required to calculate the streamer charge (appears in Chapters 3 and 6)
k		A constant that depends on the electrode shape and atmospheric conditions used in equation (3.4)
K		The total number of segments of the leader in Gallimberti's equation (appears in Chapters 3 and 6)
$L_L(t)$	[m]	The length of the leader channel at time t
L	[m]	The length of the parallel streamers used in Goelian and Lalande's approximation
L_l	[m]	The leader channel length
N		The number of parallel streamers assumed by Goelian and Lalande's model
N	[particles/m^3]	The molecular density
n_i	[particles/m^3]	The density of neutral molecules at a particular time.
n_{0i}	[particles/m^3]	The initial density of neutral molecules
P_0	[Pa]	Atmospheric pressure at 20 degrees C and at sea level
P	[Pa]	Pressure
$p_i(t)$		The probability distribution for the inception of corona
$p_e(t)$		The probability distribution of a primary free electron being in the vicinity of the electrode tip
ΔQ	[C]	The total electric charge of any streamer burst
Q	[C]	The electric charge
Q_s	[C]	The critical electric charge of the streamer and the stem zone
q_L	[C/m]	The charge per unit length required to transform the streamer into a new leader segment
R	[m]	The radius of the sphere in the rolling sphere method
R		A constant that depends on the electrode configuration in the Rizk equation (eq. 2.1)

S	[m]	The final jump distance
T	[s]	Time
T	[K]	Temperature
T_{front}	[s]	The front time of the switching impulse voltage waveform
U_C	[V]	The continuous leader inception voltage
$U_{c\infty}$	[V]	A constant that depends on the electrode configuration in the Rizk model
U_1	[V]	The potential profile after the first leader has advanced
U_{tip}	[V]	The potential at the tip of the leader channel
U_1	[V]	The voltage induced by the downward leader defined by the Rizk equation (eq. 2.1)
V_{max}	[V]	The maximum voltage applied in the switching impulse
x_0		The relationship between the leader velocity v and the leader time constant Θ using the Rizk leader equation (eq. 3.2)
z_0	[m]	The height of the leader tip above the ground for the Cooray equation (eq. 5.3)
α	[·]	The angle of protection defined by the protective angle method
β		The factor function of the return stroke current related to the transmission line voltage in the electro-geometrical method
Δl_i	[m]	The length of the new segment by which the leader channel has advanced
$\Delta L(t+dt)$	[m]	The total length of the leader channel at the time $t + dt$
ΔU_L	[V]	The potential drop across the segment of the leader
ε_0	[F/m]	The permittivity of vacuum
γ		The ratio between the heat capacity at constant pressure and the heat capacity at constant volume
θ	[°]	The angle of deviation determining the tortuous behavior of the leader channel

Abbreviations

FEM	Finite element method
LTE	Gallimberti's local thermoequilibrium equation
CSM	Charge simulation method
NC	Negative streamer
PL	Pilot leader
SL	Space leader
NL	Negative leader

1 Introduction

"*The greatest enemy of knowledge is not ignorance;*
it is the illusion of knowledge."

Stephen Hawking

For some years the insulation and lightning protection designs of high and extra high voltage equipment have been based on experimental tests and have made use of equations derived from experiments. Global population growth and the increase in industrialization throughout the world have increased the demand for electricity, which has led to a search for energy sources in remote places. In consequence, greater demands are imposed on the network of electrical power systems, and the need to transport electricity long distances more efficiently has increased. For all of the above reasons, it has become necessary to develop and design equipment for operation at electric field levels higher than ever reached before, and at which the equations developed in the past are no longer applicable. Thus, it has become necessary to understand the physics behind the discharge phenomena to make it possible to face these new challenges and to bring about technological advance. As a result of this, several experimental and numerical scientific works have been dedicated to the study of discharges in long spark gaps under different voltage stresses, electrode configurations and polarities.

Experimental studies have been used to develop empirical and physical models based on experimental formulations and, together, these have led to improvements in the electrical design of high voltage apparatus and insulation distances, but they cannot take into account factors associated with fundamental physics and/or the behavior of materials. The physical models are used to describe the discharge phenomena and to predict the behaviour of the observable properties of lightning and laboratory discharges. However, because of the complex simulations necessary to reproduce real cases, they are not in widespread use in the engineering of practical applications. Additionally, there are still many unanswered questions about the theory of discharge development, both for laboratory tests and lightning physics, and the parameters required to fit the models.

Hence, it is necessary to continue working on the methods developed to reduce the number of unproved hypotheses and to validate and complement the engineering models used. For these reasons, the aim of the work presented here was to study the breakdown process in long gaps under positive and negative polarity and the initiation of positive leaders from grounded structures under the influence of downward moving negative lightning stepped leaders; a process known as the lightning attachment process.

Chapter 2 contains a brief summary of the current knowledge about positive discharges, including, in particular, the physics and the models underlying them. **Chapter 3** and **Papers I** to **VIII** are entirely dedicated to determining a reliable model to calculate the breakdown phenomena in long spark gaps under positive switching impulses by means of the physics of the discharge. The first section starts with a presentation of a simplified methodology; from the said methodology, it was observed that one of the main parameters required in the simulation process is the characteristic of the streamer region. Generally, this is obtained by considering the streamer region to be a geometrical region with a constant geometrical shape during the complete discharge process. Later, to simplify the procedures, the streamer region was approximated by a constant, K, called the geometrical constant.

When a switching voltage is applied to an electrode arrangement (i.e., a high voltage and a grounded electrode), the background electric field changes with time. Thus, if the background electric field is modified, the streamer zone could extend over a larger or a smaller area. With the aim of reducing the number of assumptions required in the calculation of long gap discharges under switching impulses, a new model was developed and presented in Section 3.2. In **Paper VII** the methodology was introduced and is compared with other authors' propositions; **Papers V, VI** and **VIII** present the results of the application of this streamer calculation to a complete calculation of long spark gaps.

With the intention of describing the electrical potential of the leader, two alternative formulations were compared; a description of this comparison is presented in **Chapter 3** and **Paper IV**. Statistical delays have been included to reproduce the time taken by the inception of corona and, based on laboratory tests, Gaussian approximations were found to describe the tortuous behaviour of the discharge channel.

Several ultra high voltage tests performed at ABB Ludvika were simulated for two different configurations: sphere-plane and rod-plane to validate the long spark gap methodology proposed in **Chapter 3**. The results are summarized in **Chapter 4**; good accuracy was obtained for the breakdown voltage and the time to breakdown.

Chapter 5 and **Papers IX** and **X** are concerned with the first attempts to reproduce negative leader discharges under switching impulses. The existing work on the simulation of negative switching discharges had been held up by the lack of experimental data and by the fuzzy understanding of the physics involved. In the scientific community, it is well known that most of the discharges that occur in nature are of negative polarity and, because of their complexity, the only way to understand them is to generate the discharges in laboratories under controlled conditions. The waveshape applied to this problem in laboratories is a negative switching impulse. An electrostatic approximation of the negative leader discharge process is presented with the intention of applying the available information to a more realistic method than has been done previously. The simulation procedure takes into consideration the physics of positive and negative discharges, considering the negative leader to be propagating towards a grounded electrode and the positive leader to be propagating towards a rod electrode.

Most of the knowledge gained on the physics of long spark gaps under switching impulses has been incorporated in the development of models on lightning attachment. During recent years, Uppsala University has been working to develop a consistent model to simulate positive upward leaders and the process of lightning attachment. Consequently, one implementation of a lightning attachment model is included in **Chapter 6** and **Papers X** to **XIV,** in which attention is paid to the international standards implemented to protect structures against lightning. The standards on lightning protection design suggest different methodologies which are based on empirical methods or equations.

Chapter 6 and **Papers XIII** and **XIV** deal with the effect of having multiple upward leaders developing from grounded structures. Whenever an upward leader is incepted on a structure, other upward leaders can be incepted if the conditions of the electric field allow it. The newly incepted upward leader can influence the background electric field and the evolution of the lightning attachment process.

2 The behavior of positive switching impulses in long spark gaps

For years the designers of external insulation for extra high voltage and ultra high voltage transmission systems have been interested in understanding the electrical and physical behaviour of the discharges to enable them to coordinate the insulation system and the electrical protection, and to achieve the optimal design for the equipment. A first approach to understanding the electrical discharge phenomena has been made by conducting experimental studies. Furthermore, equations and numerical models have been proposed incorporating the experimental data obtained in the laboratory.

In 1971 Les Renardieres' Research Group [1] was entrusted with the task of understanding the physics underlying long spark gaps, and the different parameters involved in the breakdown process, based on an experimental programme. The experimental work consisted of performing a systematic variation of the different conditions relating to the discharge, such as changing the applied voltage (by introducing positive and negative switching impulses with a range of rise times, fall times and maximum magnitude), and using various electrode configurations and gap distances. Once the experimental results had been obtained, the data was divided among the scientists, enabling different approximations and models to be proposed [2- 4].

One of the greatest contributions of Les Renardieres' Group was to identify the fact that positive discharges are composed of two parts: the leader channel and the streamer zone. This research enabled them to describe the complete discharge process right up to the instant at which the breakdown took place. From the experimental data collected by Les Renardieres' Group, different models have been proposed. Some of them are known as engineering models, which are approximations or equations fitted to the experimental data; these include models such as the critical radius concept of Carrara and Thione [5], the leader intensification criterion of Petrov and Waters [6] and the leader inception voltage concept of Rizk [7- 9]. With the evolution of the computational software and hardware capacity, more complex numerical models have been developed, most of which are based on the detailed compendium written by Gallimberti [10] and the leader-streamer model which was the result of collaborative work, published by Bondiou et al [11]. Some

of the leader inception models based on the real physics of the discharge are Lalande's upward leader models [12], Goelian and Lalande's simplified approximation [13, 14] and Becerra and Cooray's model [15].

After the Les Renardieres' Group work, the interest of the scientific community focused on the application of the numerical equations and methods developed to areas such as rocket-triggered lightning, lightning protection, and lightning attachment. Nowadays, most of the numerical models that are presented to the scientific community have been validated using the results obtained by Les Renardieres' Group.

As far as the consideration of the breakdown behaviour under switching impulses is concerned, the industrial sector is still performing a variety of experimental tests to facilitate the design of equipment and substations, because the theoretical methods developed to date are incapable of predicting breakdown voltages and times to breakdown under different electrode configurations. In addition, the available methods are time-consuming and they have several input parameters to which the models are highly sensitive and which need to be changed for each different spark gap configuration.

The lightning attachment models [14, 15] have been validated first through the laboratory work of the Les Renardieres' Group [1] and subsequently through the experimental work conducted with rocket-triggered lightning [14], but they have assumed several parameters that also need to be validated.

2.1 The mechanism underlying positive leader discharges

The mechanism underlying long air-gap discharges was the first attempt to provide a theoretical explanation for the physical observations and was based on the application of switching impulses to a high voltage electrode-plane arrangement by Les Renardieres' Group [1, 2] and the physical explanation of the data presented in the references [10, 16, 17]. The process starts with the appearance of a bunch of filaments called streamers or the streamer zone at a point in time, designated t_1, developing from the high voltage electrode. Continuing the analogy of the bunch of filaments, it is possible to observe a region that is illuminated in the root area of the streamer, which reveals the path along which the leader channel forms. The charge located in the streamer zone reduces the local electric field over the tip of the high voltage electrode. However, the reduction of the electric field brought about

by the streamer charge is compensated for by an increase in the voltage at the high voltage electrode, which increases the electric field. Then it is followed by a period characterised by the absence of light, a so-called dark period.

At t_2, as shown in Figure 1, the simultaneous development of a leader channel and a second streamer takes place. The first leader segment is called the "stem" and it is determined by the following two criteria [10]:

- The combined current of the first corona streamers passing through the root of the first corona burst will cause heating of the gas. If the temperature rises to 1500 K, the detachment of negative ions will take place producing an increase of electrons in the medium, and thus increasing the plasma conductivity. As a result of this, this zone becomes highly conductive and increases the electric field at the high voltage electrode.
- The electric field at the extreme of the stem (the closest point to the grounded electrode) should be high enough to allow the formation of another stem and a second streamer.

This transition from streamer to leader is called unstable leader inception, and it is brought about when the total charge ΔQ in the second streamer is equal to or larger than about 1 μC [10]. After the time t_2, a system composed of a leader channel and a streamer zone at the head of this leader channel starts to evolve; this stage is called the "*Leader – Streamer*" stage. The evolution of this "*Leader – Streamer*" is highly influenced by the rise time of the applied switching impulse. When the rise time is fast, the propagation of the discharge is continuous, and when it is very slow, the propagation is discontinuous. When the energy available at the front of the leader tip is high enough to sustain the thermalization of the channel and the creation of new leader segments, the leader starts to propagate continuously with streamers developing at its tip. This condition defines the stable leader inception.

During the propagation, the leader advances with a velocity of 10^4 m/s and it is supplied at its end by an average current of 0.5 to 1 A [3, 17].

The final stage of the leader propagation or the "*final jump"* is produced when the streamer zone of the leader reaches the opposite electrode. In this stage the leader is accelerated from a velocity of the order of cm/μs to m/μs.

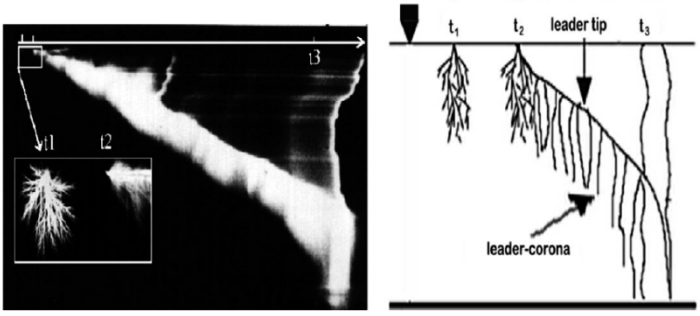

Figure 1. A streak image and sketch of the development of the positive leader discharge in a laboratory long air gap with a 10 meter gap, t_{front} = 500 μs and V_{max} = 2.5 MV (adapted from [17] with permission of Elsevier).

2.2 Leader inception models

Based on the experimental data and the previous physical details analyzed by Gallimberti [10, 17] and Les Renardieres' Group [2], different equations and numerical models have been developed to calculate the leader inception voltage. The models have been validated with the measurements from the Les Renardieres' Group and good agreement has been obtained. The models and the equations obtained for the propagation have been extrapolated for use on lightning and, nowadays, are well-known concepts used in the design of the lightning protection of grounded structures.

The knowledge gained about the mechanism of the discharge in air has facilitated the improvement of engineering models for the prediction of breakdown in gaps, such as the Golde's criterion [18, 19], and the models of Lemke [20], Alexandrov [21], Jones [22], Hutzel [23], and Bazelian [24]. These models do not enter into detail on physical aspects of the phenomenon, but they utilize a large amount of information, qualitative and quantitative, gained on the characterization of each one of the phases of the discharge mechanism. A brief description of them can be found in Arevalo's work [25].

Other models tried to approach the physics of the phenomena through laboratory experiments, by identifying equations for the leader channel and the streamer region, such as those of Carrara and Thione [5], Rizk [8-9, 26] and Dellera and Garbagnati [27- 28], and Petrov and Watters' criteria [6].

A concept widely known as "the critical radius concept" was proposed by Carrara and Thione [5] and is now in widespread use. The model was built

up from observations on rod-plane and conductor-plane configurations under positive impulses with a critical front. The model has been extensively applied to phase-to-ground and phase-to-phase configurations, finding good agreement between the computed and the experimental results. Nevertheless, the study extended by the Les Renardieres' Group [3] for the same configurations with other voltage waveforms found that the value of the critical radius changes for different values of the time to crest for the applied voltage.

The critical radius principle was first used on lightning studies by Eriksson [29]. Since then, it has generally been applied to compute the leader inception conditions in rods, masts, power lines [7, 8, 26-28, 30, 31] and in buildings [32]. As a result, any sharp point on a structure, such as the tips of lightning rods, corners or edges, is rounded off to the critical radius to minimize the probability of a lightning strike, and it is assumed that a stable leader is initiated when the electric field on the surface is equal to the critical streamer inception electric field (about 3 MV/m).

A more physically realistic model was presented by Rizk [8, 26], whose model introduces the criteria for leader inception and the breakdown voltage of different electrode configurations under positive switching impulses with a critical time to crest. It takes into account the conditions of the leader and the conditions for the final jump. The zone containing the streamer and stem are characterized by the critical charge Q_s and the lengths of the leader channel and the air gap. This condition is satisfied under impulse voltages that increase, keeping the potential at the leader tip approximately constant as the leader propagates in the gap. The model results in expressions for the continuous leader inception voltage U_C for different gap configurations:

$$U_C = \frac{U_{c\infty}}{1+\frac{A}{R}} \tag{2.1}$$

where A, $U_{c\infty}$ and R are magnitudes that depend on the electrode configuration. The model shows a good agreement with the experimental results. The application of this model to air density effects is reported in the work of Rizk [26, 9], where it is proposed that a continuous positive leader is initiated from any grounded structure of height h when the voltage U_1 induced by the downward leader and/or the thundercloud at a height h in the absence of the structure is equal to:

$$U_1 = \frac{U_{c\infty}}{1+\frac{A}{h}} \tag{2.2}$$

The values of the constants A and $U_{c\infty}$ have been determined for rods, tall masts and transmission lines [9]. The results of this model are based on laboratory data pertinent to switching impulses and it is doubtful whether they are also valid in the case of electric fields generated by stepped leaders. Moreover, the results are valid for isolated conductors which make its application more restricted.

Another model was proposed by Dellera and Garbagnatti. This model involves the simulation of the propagation of positive and negative leaders from data based on electrostatic calculations. The model is known as the leader progression model. In this case, the downward leader is modeled by a line with a given charge density, which is a function of the prospective return stroke current, while the upward leader is represented by line charge segments of constant density. The attachment of the downward leader to a grounded structure was computed from the calculated striking distance and the relative velocity ratio of both leaders. The criterion for leader inception used is the critical radius concept [5].

Petrov and Waters [6] have developed a leader inception criterion, which assumes that when the streamers from the electrode extend beyond a critical length equal to 0.7 m, positive upward leaders can develop. The electric field over the streamer zone must exceed a critical value of 500 kV/m. However, laboratory experiments with long sparks in the rod-plane configuration have shown that the critical streamer length for unstable leader inception is equal to about 3 m [4]. This latter criterion was used by Akyuz and Cooray [33] to study lightning attachment to Franklin rods. The model of Petrov and Waters was extended in research conducted by D'Alessandro and co-workers [34] by assuming that the stable propagation of the incepted leader is reached if the rate of change of the potential induced by the downward leader at the rod's tip is larger than 6 kV/μs.

Other physical models delve deeply into the particles' behavior, like Bondiou and Gallimberti's model [11], which introduced the basic physics principles, and other authors' work, like that of Lalande [12], Goelian et al [13], Castellani [35], and Becerra and Cooray [15], where modifications were made to the model introduced by Gallimberti [10] and in which lightning attachment processes or the breakdown in long gaps were calculated. The assumptions underlying the streamer calculation are different in each model, as described in the following paragraphs:

Bondiou and Gallimberti's model [11] calculates the charge generated by the streamer formation in terms of estimating the total number of electrons that have left the gap by reaching the high voltage electrode. The calculation takes into account the attachment process. However, as a simplification, the

charge is assumed to come from a single filament, therefore the charge for the total streamer area is estimated by multiplying the charge from a single streamer by a branching factor and by the number of filaments. In this procedure, the constants used for the first streamer and all subsequent streamers are the same.

A simplified model for the simulation of positive sparks was developed by Goelian and Lalande's model [12, 13] calculates the charge associated with the advancement of the streamer-leader by multiplying the area formed by the potential distribution immediately before and after the streamer formation by a geometrical constant. For the calculation, the streamer area is assumed to be comprised of N parallel streamers of length L, located at a distance a_i from each other. The charge simulation method is then used to evaluate the electrical charge from the area covered by the leader between the potentials at two different instants of time and the representation of the N linear streamers.

The Becerra and Cooray streamer approximation [15, 36, 37] assumes that the area covered by the streamer zone required for the simulation process is conical. The charge accumulated is calculated by means of the charge simulation method. In the most recent version, Becerra and Cooray [36] proposed a simplified method in which the area accumulated between the potential of two consecutive leader segments is proportional to the streamer charge. The proportional constant used to calculate the charge is called the geometrical constant K.

The last three methodologies mentioned above presumed that the leader advances by segments and each segment is characterized by the thermo-equilibrium equation of Gallimberti [10]. The charge per unit length required to achieve the transition to a new leader segment in the case of the models of Bondiou and Gallimberti [11], Lalande's [12] and Becerra and Cooray [15] is derived from thermodynamic analysis of the transition region where the streamer converges on the leader tip [10].

3 A simplified and a complete methodology to calculate the breakdown process in long spark gaps under positive switching impulses

A new and simplified methodology for the calculation of breakdown voltages and the time to breakdown in long spark gaps is presented in **Papers I** and **IV**. It is based on the previously described physical methodologies and the well-known "streamer-leader" model [11]. **Papers II** and **III** concern the application of the methodology mentioned.

After analyzing the advantages and disadvantages of the different methods it was determined that the most critical part of the calculation is that for the streamer. Therefore, two electrostatic approximations for calculating the streamer region are presented in **Paper VII** and the implementation of one of them to the long spark gap methodology is presented in **Papers V, VI** and **VIII**.

3.1 Simplified methodology for the simulation of long spark gaps

The simplified model has been modified, mainly in the calculation of the leader channel where two different models were implemented and compared. For all of the cases simulated, the model used the finite element method software COMSOL® to calculate the electric field and the potential distribution between the high voltage electrode and the grounded electrode. For the input of the physical equations and routines, Matlab ® was employed.

3.1.1 The initial methodology

In **Paper I**, a non-probabilistic methodology is presented. The calculation is divided into two main parts, one for the streamer zone and the other for the leader channel. The streamer zone was modeled using the geometrical ap-

proximation of Lalande [12] (see equation 3.1). The leader channel was modelled using Rizk's equation [7], which is an approximation taken from long gap experiments [2].

The streamer charge is calculated using the following equation:

$$Q = K \cdot 4 \cdot \pi \cdot \varepsilon_0 \cdot \int_0^{Z_s} (U_2 - U_1) \cdot dz \qquad (3.1)$$

where $(U_2 - U_l)$ is equivalent to the potential change attributable to the streamer charge region and K is a geometrical factor introduced by Lalande [12, 13].

In contrast to previous methodologies, the model supposes that the ionization process is generated in the zone between the leader and the front of the streamer, which is in direct contrast to the presumption made in the model of Bondiou and Gallimberti [11], which supposes that the ionization process only takes place in the head of the streamers. In Figure 2, dashed lines can be seen representing the area assumed to be the new region after the time $(t+dt)$.

Rizk's equation is applied, for the calculation of the leader channel, which established that the voltage at the tip of the leader is a function of the leader length L_l, the electric field in the streamer zone E_{sc}, the final quasi-stationary leader gradient E_∞ and the relation x_0, which is the relation between the leader velocity v and the leader time constant Θ

$$U_{tip} = L_l \cdot E_\infty + x_0 \cdot E_\infty \cdot \ln\left(\frac{Esc}{E_\infty} - \frac{Esc - E_\infty}{E_\infty} \cdot e^{-\frac{L_l(t)}{x_0}} \right) \qquad (3.2)$$

The advancement of the leader channel is calculated using the equation

$$\Delta l_L^{(i)} = \frac{\Delta Q^{(i)}}{q_L} \qquad (3.3)$$

where q_L is the charge per unit length required to cause the transformation of the streamer located in the active region in front of the already formed leader channel into a new segment of the leader. The magnitude of q_L is based on the observations made by Les Renardieres' Group [2]

The methodology presented in **Paper I** makes a simplification of the calculation of the background potential for each time step. The potential is calculated only once with FEM in per unit scale, and for the next time-step, the

curve obtained is scaled up as the potential increases in the high voltage electrode.

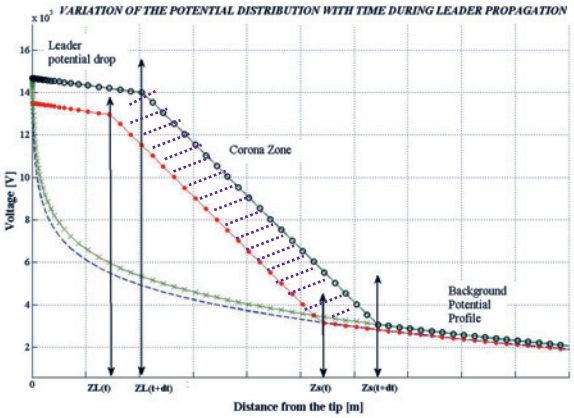

Figure 2. Representation of the potential distribution variation for two different time steps. The background potentials are represented by green and blue lines, the leader potential drop using Rizk's equation (3.2) and the streamer zone as a constant electric field of 500 [kV/m]. The charge necessary for the next time step corresponds to the dashed line.

The methodology was compared with the experimental results presented by Les Renardieres' Group [1], and with the results presented by Lalande [12], Goelian et al [13], and Becerra and Cooray [15]. Good agreement was observed between the existing models and the proposed methodology.

3.1.2 The statistical variations

The time at which an electrical discharge is initiated is uncertain and dependent on many unknowns, which introduces one source of statistical dependence. Another source is introduced by the tortuous nature of the path taken by the discharge. One statistically dependent source of time delay associated with breakdown corresponds to the combined effect of every elementary process that the discharge needs to develop before breakdown can occur, and the other arises from the random nature of the path the discharge takes to reach the ground. In **Paper II**, the statistical variations mentioned here are incorporated into the model. A brief summary of **Paper II** is presented in the following paragraph.

The first source of time delay corresponds to the random nature of the corona inception, which requires a primary free electron in the vicinity of the electrode tip which is capable of initiating an ionization process. The proba-

bility distribution for inception was taken from the critical volume region of corona proposed by Baldo [16]:

$$p_i(t) = p_e(t) \cdot \exp\left[-\int_0^t p_e(t)dt \right] \quad (3.4)$$

$$p_e(t) = k \cdot V(t) \cdot t \quad (3.5)$$

$$\sigma_{T_i} = \frac{1}{2 \cdot \sqrt{k \cdot V(t)}} \quad (3.6)$$

In the above equations $p_i(t)$ is the probability distribution for the inception of corona, p_e(t) is probability distribution corresponding to a primary free electron being in the vicinity of the electrode tip, *V(t)* is the variation of the potential with time, and *k* is a constant that is determined by the electrode shape and atmospheric conditions, which was calculated from measurements conducted by Les Renardieres' Group [2].

Initially, to represent the random behavior of the leader channel, experimental measurements of the tortuosity of lightning discharges made by different researchers were used [3, 38-39]. A Gaussian distribution with a mean value of 15 degrees and a standard deviation of 11 degrees was selected to represent the tortuous path. For every segment of the leader, a random selection of the angle from the Gaussian distribution was calculated, therefore each resultant segment has a magnitude *dl* and an angle Θ, as shown in **Paper II**.

The advance of each successive leader segment was calculated from the following equations:

$$\Delta l^{\prime} = \frac{\Delta Q}{q_L} \quad (3.7)$$

$$\Delta l = \Delta l^{\prime} \cdot \cos\theta \quad (3.8)$$

$$\Delta L(t + dt) = L_L(t) + \Delta l_l \quad (3.9)$$

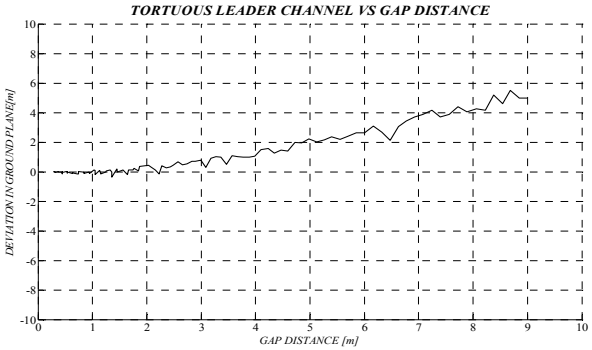

Figure 3. Tortuous leader channel obtained in one of the simulations after the geometric projection of the vector *dl* onto the straight path, where the potential distribution was solved using COMSOL ®

With the intention of evaluating the methodology including the statistical variations, a constant level test was simulated to obtain the 50% breakdown voltage and the 50% time to breakdown. A comparison was made and the results are presented for a tortuous leader path and a straight path. As shown in **Paper II**, the breakdown voltage is not affected by the tortuous behavior of the leader channel, however, the time to breakdown changes with the tortuosity of the channel. Table 1 is constructed from the data presented in **Paper II**; it can be seen that the channel tortuosity changes the time to breakdown of the discharge.

Waveform	***50% Time to Breakdown***				
	Measured Value	***Calculated value***			
		Straight path	***% error***	***Tortuous channel***	***% error***
500/10000 µs	552 µs	579.36 µs	4.9%	609 µs	11%
1800/10000 µs	980 µs	787.7 µs	19%	809.4 µs	17%
2200/10000 µs	1183 µs	943.3 µs	3%	953.4 µs	19%

Table 1. Comparison of the time to breakdown using a straight discharge channel and a tortuous discharge channel

The percentage error is smaller when a straight channel was used for the simulations than when a tortuous path was assumed. This high percentage

error arises because the normal distribution used for the tortuous path is based on lightning measurements owing to the lack of information available on tortuous leader channels in long spark gaps under switching impulses.

Analyzing the effect of the leader direction, it can be observed that the change of direction generates a reduction in the leader velocity. Therefore, the breakdown might be delayed, i.e., the time to breakdown of the discharge is increased.

3.1.3 Comparison of the equations for two different leaders

With the aim of improving the model by making a more physically realistic approximation, two different leader models were implemented in the simplified methodology and the behavior of the models was compared. **Papers III** and **IV** present the results obtained and the comparison of the models, respectively.

The first leader criterion used was the Rizk engineering approximation [7] assuming tortuous and non-tortuous leader paths. Gallimberti's concept of "local thermodynamic equilibrium" [10] was implemented to introduce a more physically realistic approach to the voltage drop along the leader channel.

With Gallimberti's approach the leader was decomposed into elementary segments of length dl, temperature T, pressure P and with a molecular density n that is uniform along the channel. In this instance, the potential drop ΔU_L in the segment i will be:

$$\Delta U_{Li} = E_{Li} \cdot dl_i \qquad (3.10)$$

where dl_i is the length of the segment i and E_{Li} is the potential gradient of the segment of length i.

Gallimberti's model gives the evolution of the internal electric field E_L as a function of the current injected, calculated under the supposition that the conductivity of the leader channel is essentially controlled by electronic collisions between neutral molecules and electrons accelerated in the electric field E_L. It supposes that all the injected current I_L is used to extend the leader and the expansion is made with a constant mass. The formulation describing this hypothesis results in the following set of equations:

$$\pi \cdot a_{0i}^2 \cdot n_{0i} \cdot dl_i = \pi \cdot a_i^2 \cdot n_i \cdot dl_i \qquad (3.11)$$

$$\frac{\gamma \cdot p_0}{\gamma - 1} \cdot \frac{d\left(\pi \cdot a^2\right)}{dt} = E_L \cdot I_L \qquad (3.12)$$

where a_i is the radius of a leader segment at a particular instant in time, n_i is the density of the neutral molecules at the same instant and a_{0i} and n_{0i} are the initial conditions required for the leader formation. P_0 is atmospheric pressure, γ the ratio between the specific heats at constant pressure and volume, $d(\pi a^2)$ is the variation in the cross-section of the leader, and $E_L\, I_L$ is the power injected into the channel during a time step dt.

From equation (3.11), it is possible to calculate the channel section for the next time step as a function of time at the time t, and the internal electric field and the charge $I_L\, dt$

$$\pi \cdot a^2 \cdot (t + dt) = \pi \cdot a^2(t) + \frac{\gamma - 1}{\gamma \cdot p_0} E_L \cdot I_L \cdot dt \qquad (3.13)$$

As the mass from the molecules is constant, the density can be written as:

$$n(t + dt) = n(t) \frac{\pi \cdot a^2(t)}{\pi \cdot a^2(t + dt)} \qquad (3.14)$$

And, using the hypothesis that the ratio E_L/n is constant, the internal electric field as a function of time will be given by:

$$E_L(t + dt) = \frac{n(t + dt)}{n(t)} E_L(t) \qquad (3.15)$$

Thus, it is feasible to calculate the time evolution of the internal electric field for each segment and the potential drop along the leader channel

$$\Delta U_L = \sum_{i=1}^{k} E_{Li} \cdot dl_i \qquad (3.16)$$

where k is the total number of segments.

As the goal was to improve the calculation by adopting a more realistic approach than had previously been taken, in **Papers III** and **IV,** the electric field in the gap was recalculated for every time step, taking into account the new leader segment and the voltage applied to the high voltage electrode. The models were compared by conducting three different tests: one was a deterministic simulation performed with Rizk's equation and the "Local Thermoequilibrium, LTE" equation of Gallimberti's, presented in **Paper IV**. Another was a statistical simulation including an up-and-down test, presented in **Paper III,** and a constant level test for different peak voltages for a positive switching impulse waveform 500/10000 μs applied to the rod elec-

trode which is discussed in **Paper IV**. The simulations were made using the Les Renardieres' Group laboratory configuration [1]. The characteristics of the setup are a 10 m point-plate with a 10 mm radius cone at the tip, forming the point.

In **Paper IV** and Figure 4, the results for a deterministic calculation are presented, i.e., without statistical variations and by making a simplified calculation of the streamer zone, the breakdown conditions using the LTE equation are fulfilled faster than using Rizk's equation. It is important to mention here that Becerra and Cooray [15] simulated the long gap discharges using the same set-up as Les Renardiers' group [1] using their own model, which is also based on the physics described by Gallimberti [10]. They found good agreement with experimental data, however, in their calculation, they evaluated the charge in the streamer zone by using the charge simulation method for each time step. This procedure was not used in the present engineering application because the aim of this part of the research was to evaluate and analyze a simplified calculation avoiding a large number of computations.

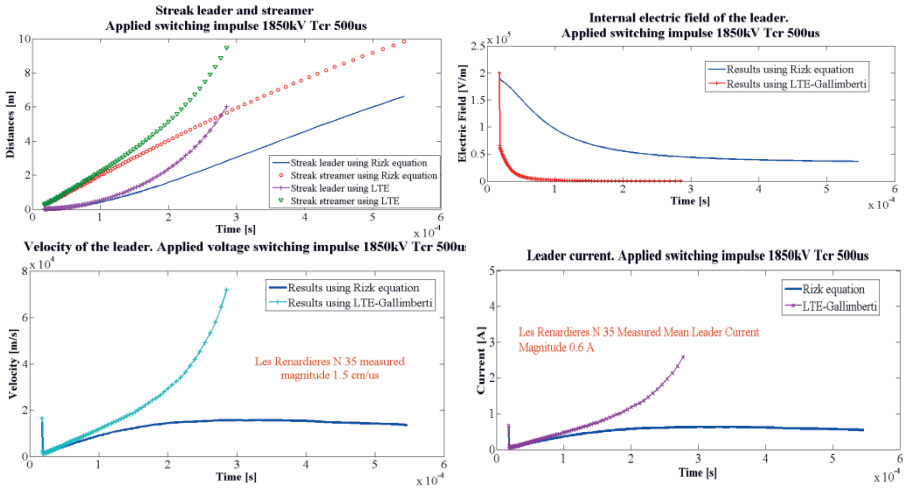

Figure 4. Numerical simulation of the propagation of the positive discharge in a point-plate laboratory configuration. Comparison between Rizk's equation and the LTE equation. From left to right and top to bottom, the figures presented are: a streak image of the leader channel, the internal electric field of the leader channel, and the velocity and current of the leader channel. Reproduced from **Paper IV**.

The resulting accuracy of the engineering model was improved by using the "LTE equation of Gallimberti", in conjunction with the statistical distributions representing the corona inception and the tortuous leader channel. The

results showed that the mean value of the leader current and the velocity agree best with the experimental results, as can be observed in Figure 5.

From the results obtained with the statistical simulations performed with the LTE equation of Gallimberti's and the Rizk equation, it is possible to conclude that the time to breakdown and the leader characteristics are quite close between both leader criteria. It is important to outline that Rizk's equation was deduced from Les Renardieres' Group results [1, 3], therefore it is only to be expected that good agreement would be obtained with this equation. Meanwhile, Gallimberti's LTE equation, together with the other approximations used in the procedure, need to have statistical variations incorporated for the path taken by the discharge to give the correct results.

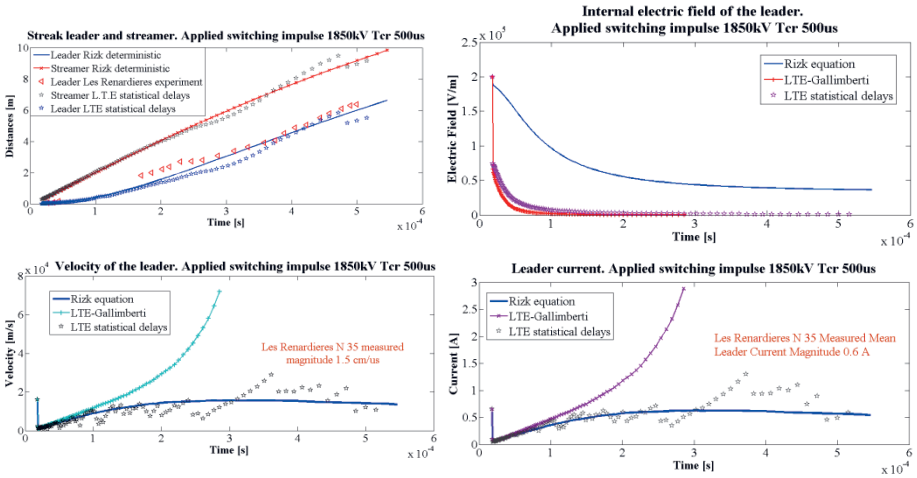

Figure 5. Numerical simulation of the propagation of the positive discharge in a laboratory using Gallimberti's LTE equation with statistical delays incorporated to represent the inception of the streamer and the path of the discharge. Taken from **Paper IV**.

As an application of the model, an up-and-down test and a constant level test were simulated. The results are presented in **Papers III** and **IV**, respectively. The breakdown probability at different voltage levels and different waveforms is computed, but unfortunately the values obtained cannot be compared with experimental data since the experimental data available in the literature is sparse.

The contributions made up to this point to improving the calculation can be found in **Papers III** and **IV** and can be summarized as follows:

- The leader channel was simulated to obtain a more physical approach using Gallimberti's thermoequilibrium equations [10].

- Two statistical variations were implemented, one for the inception of the corona, and the other to describe the tortuous nature of the leader channel.
- For every leader segment, the background electric field was recalculated, in contrast to the method used in **Papers I** and **II** and discussed here on pages 31 to 36.

3.2 Full version of the long spark calculation for a variable streamer region

To improve the methodology proposed for the calculation of long sparks, one must analyze the sensitivity of the input parameters to calculate the streamer region and estimate the effect of the simplified method used to compute the streamer zone. Authors have assumed certain physical factors, like the distribution of the electrical charge, to simulate the streamer region of the discharge and, in general, this has been achieved by representing it as a region with a constant geometrical shape. Different geometries have been used, such as cones [15] or several parallel filaments [12, 13] to determine which best reproduces the experimental data.

However, when a switching voltage is applied to an electrode arrangement (comprised of a high voltage and a grounded electrode), the background electric field varies with time. Thus, if the background electric field is modified, the streamer zone could cover a different volume.

With the aim of reducing the number of assumptions required in the calculation of long gap discharges under switching impulses, a new means of representing the streamer region was presented in **Paper VII**, and practical applications of this model to the long-gap calculation methodology were made in **Papers V, VI** and **VIII**. This model considers a variable streamer zone that changes with the electric field as was described in **Paper VII**. The three dimensional region that fulfills the streamer condition is identified for each time step, and the charge accumulated in that region is then calculated. The only assumption made in the calculation is the minimum electric field of the streamer region.

The leader channel was modeled using the local thermoequilibrium model of Gallimberti [10], with the streamer zone being located in front of the leader and the statistical variations arising from the inception and tortuous nature of the leader channel being included. For comparison purposes, different gap configurations [1, 11, 40, 41] were simulated and their results are presented

in **Papers VI** and **VIII**. The outputs of the model agreed well with published experimental data.

3.2.1 Methodology

A detailed description of the calculation procedure can be read in **Papers VI** and **VIII**. Here, instead, brief explanations of the novel implementations introduced in the calculation are described in the following paragraphs, where reference is made to the relevant publications.

3.2.1.1 **Streamer Region**

Two methodologies were implemented to calculate the streamer region, and they are discussed and compared in **Paper VII**; only a brief description is given here

Procedure 1

The calculation was divided up into four specific steps:

1. Once the avalanche has developed into a space charge cloud of positive ions, the local field may be high enough to start a new avalanche closer to the cathode. Whether or not this process continues until the cathode is reached depends on the applied electric field strength. The lowest value at which stable propagation appears to be possible is called the stability field, E_{st} [10]. Its characteristic value in ambient air is between 400 and 500 kV/m [10, 11]. It has been shown from the theory that the field inside the streamer channel, is equal to the stability field [10, 42-43].

   As the stability field is equal to the field inside the streamer channel, the volumetric region between the tip of the leader channel/or the high voltage electrode and the ground point is divided into several layers. For each layer, the area where the field is equal to or higher than the stabilization electric field (assumed here as 450 kV/m) is identified.

2. In this streamer region, it is assumed that the streamers propagate along the electric field lines; the drop in the potential along the electric field line to the boundary of the region is equal to 450 kV/m. As is illustrated in Figure 6, streamers are assumed to propagate along the electric field lines, and the drop in the potential along the line is equivalent to the propagation electric field.

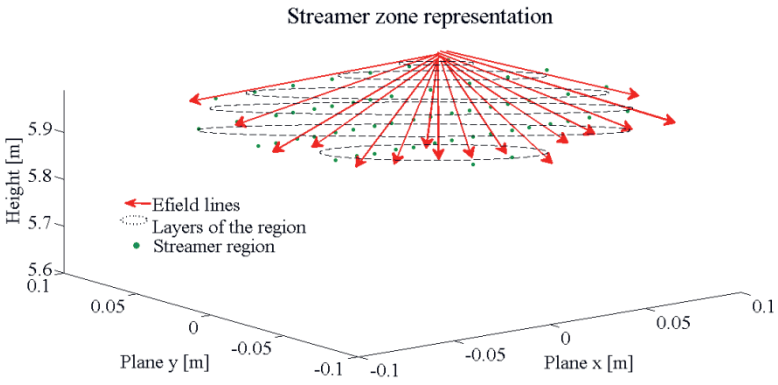

Figure 6. The geometry of the streamer region at a specific instant in time; the arrows indicate the direction of the electric field vector. The dotted red lines represent the layers for which the charge is calculated.

3. The streamer region is then divided into several layers and the charge is calculated for each layer. This calculation requires that the direction of the electric field vector be taken into consideration, including at the edge of the region.

   Using Gauss's theorem, the streamer charge located in each layer Q_i is calculated, and the total charge accumulated in the volume for each time step, Q_{total} is computed. Once the new charge has been found, the source voltage increases and the calculation to identify the new streamer region is redone.

$$Q_i = \iint_s \varepsilon_0 \cdot \vec{E} \cdot d\vec{S} \tag{3.17}$$

$$\Delta Q_{total} = \sum_{i=1}^{n} Q_i \tag{3.18}$$

Procedure 2

1. In this procedure, as in the first one discussed above, it is presumed that the streamers propagate along the electric field lines, and therefore, for each electric field line from the high voltage electrode, the respective background potential is determined, and for each potential profile, the distance at which the background potential satisfies the condition that the stabilization electric field E_{stab} is equal to 450 kV/m is found.
2. The charge is calculated using Gauss's theorem, as used in the first procedure in equations (3.17 and 3.18).

For all the calculations carried out, procedure 1 was used, because, as revealed by the comparison made in **Paper VII**, there are no important differences between the two procedures.

Figures 7, 8 and 9 demonstrate how the streamer zone changes at different points in time; the calculations presented have been carried out for the configuration used by Les Renardieres' Group [2], assuming a conical tip under a 1850 kV switching voltage impulse (500/10000 μs), and a gap space of 10 meters. Figure 7 represents the instant at which the charge started to accumulate in the region between the tip and the plane. This electric charge is located next to the tip of the leader channel, and the tip is moving away from the high voltage electrode. As can be observed, the geometrical shape of the streamer charge takes a form that is approximately conical (dashed lines).

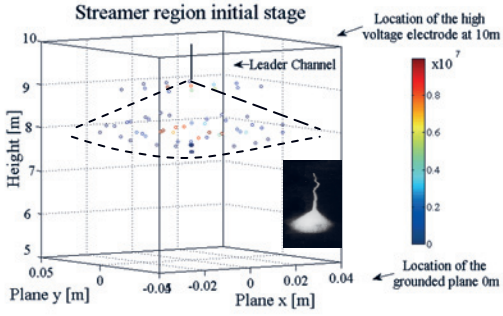

Figure 7. Streamer region in a long gap of 10 meters. Results obtained for a simulation assuming a conical tip-plane geometry. The high voltage rod is located 10 m from the grounded plane, and the latter is defined as being located at the position defined as 0 m. The small picture corresponds to a photograph taken of the same experiment.

However, when the leader channel has propagated some distance towards the grounded plate electrode, the streamer region changes shape from the conical one illustrated above to that presented in Figure 8. Once the final jump condition has been satisfied, the results showed that the geometrical shape of the streamer zone becomes easier to describe again, being more like a cylinder than the initial cone or the amorphous intermediate geometrical shape (see Figure 9).

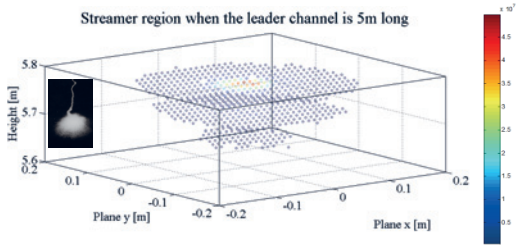

Figure 8. The streamer region in a 10 meter long gap, for a gap comprised of a rod and plane. This simulation was made when part of the leader channel had moved towards the grounded electrode. The small picture corresponds to a photograph taken of the same experiment.

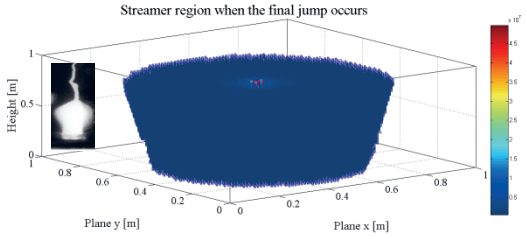

Figure 9. Streamer region in a 10 meter long gap. The results obtained are for a simulation assuming a conical tip and a plane. The grounded plane is located at the position marked 0 m, and the high voltage rod is located 10 m away from it. The small picture corresponds to a photograph taken of the same experiment, and it illustrates the leader channel and the streamer region.

The photographic results presented in a previous paper [17] are reproduced in Figure 10; they show a similar time-dependent behavior to that obtained in the simulations: Initially a conical region was observed, then a hyperboloid and, finally, the charge extends into a shape that is roughly cylindrical in form.

Figure 10. Streak image of the development of a positive leader discharge in a long air gap in a laboratory. The air gap was 10 meters, t_{front} = 500 μs and V_{max} = 2.5 MV. This figure has been published elsewhere [19] and has been reproduced with the permission of Elsevier.

The change in the shape of the streamer region under a switch-like voltage impulse in the simulations is caused by the incrementation of the voltage applied to the high voltage electrode. When the voltage source is increased, the electric field rises, and the region that will fulfill the criterion for a streamer region grows. This result reveals that the frequently made assumption of a constant geometry for the streamer region during an incrementation of the electric field disagrees with the real physical process of the discharge.

3.2.1.2 **Tortuous nature of the path**

Electrical discharges are characterized by: their random nature, taking tortuous paths and having an unpredictable inception time. These delays can be represented as statistical distributions. The above-mentioned statistical delays were included in the model to make a realistic calculation, as presented in Section 3.1; however, the statistical distributions used in Section 3.1 corresponded to different lightning measurements.

With the aim of obtaining a proper representation of the tortuous path taken by the discharge, several data from industrial tests of long spark gaps under switching impulses made at ABB/PS-HVDC were used [44, 45]; Figure 11 presents a collection of paths obtained from a series of tests.

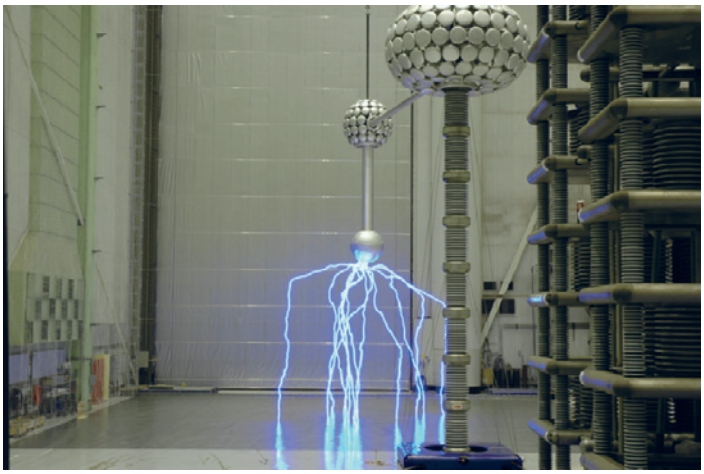

Figure 11. Tortuous path of the discharges for several laboratory tests of switching impulses made by ABB-PS/HVDC Ludvika for a long spark gap. Taken from [44].

A Gaussian distribution was determined that represents the random behavior of the leader channel in a suitable manner; it is presented in equation (3.19).

$$f(x) = a_1 e^{-\left(\frac{x-b_1}{c_1}\right)^2} \qquad (3.19)$$

Where a_1, b_1 and c_1 are constants obtained from tests conducted during the normal fitting of several long gap switching impulses. It is important to mention that it was observed that the constants in the Gaussian distribution depend on the electrode configuration; examples are presented in the following table:

Table 2. Coefficients of the tortuous Gaussian distribution with confidence intervals of 95%. distribution for different electrode configurations

Constant	Square rod	Hyperboloic rod	Sphere
a_1	3.67(3.13, 4.21)	4.03	2.33(0.69, 3.97)
b_1	0.052(-0.07, 0.18)	-0.5	0.89(-0.40, 2.18)
c_1	0.29(0.17,0.41)	1.46	1.13(-0.42, 2.68)

3.2.2 Results of the simulations

A series of methodologies was implemented for comparison purposes: the methodologies proposed by Becerra and Cooray, assuming a conical area for the streamer region and using the charge simulation method [15], the simplified method of Goelian et al [13], the simplified method presented in section 3.1, and the new method presented here in section 3.2.

The laboratory geometry used for the calculations was the one used in Les Renardieres' Group's configuration [2], which has been widely used in previous research to validate models [13, 15, 25]. In addition, to check the reliability of the methodologies for different gap configurations, the rod-rod geometry used by Paris [40] was also studied. A brief summary of the results is presented here and more details can be found in **Paper VIII**.

The first set-up was selected because all of the existing numerical methodologies have been validated using the same rod-plane electrode arrangement, making it the ideal configuration to make comparisons with. The second set-up was used because it is known that the electric field distribution of a rod-rod arrangement is different from the rod-grounded plane one. In addition, as the streamer zone depends on the electric field, it can be anticipated that the shape of the streamer zone will be affected by the differences in the electric field. Therefore, it is anticipated that the assumption of a constant streamer zone will lead to results that are not in agreement with the measurements.

The aim was to show that the proposed methodology can be used for different kinds of configurations, and to compare the results with those from other methods proposed by different authors.

Overall, from the first set-up, one can conclude that the results obtained with the different methodologies agreed with the work done by Les Renardieres' Group [2] in with respect to the leader channel position and the breakdown voltages (see Figure 12).

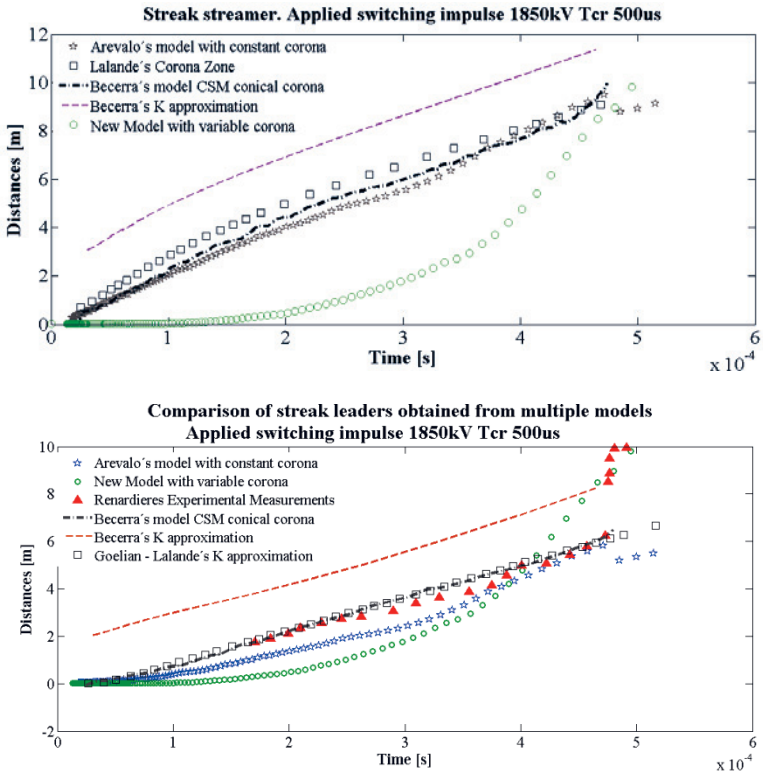

Figure 12. Streak sketch showing the development of a positive leader and the streamer discharge in the laboratory in a long spark air gap with a 10 meter gap; t_{front} = 500 µs and V_{max} = 2.5 MV.

With the purpose of determining if the methodology can reproduce different electrode arrangements, the rod-rod configuration was selected. Because the rod electrode has a termination different from the one used by Les Renardieres' Group, the configuration square rod-plane was simulated; the simulations can be seen in Figure 7 of **Paper VIII**. The results obtained using the other authors' methodologies indicate that, even though the results of the breakdown can be reproduced for a gap comprised of a rod and plane, their accuracy is not as good as that obtained with Les Renardieres' group ar-

rangement as errors greater than 20% have been obtained with them. Instead, using the methodology proposed in this research work, errors of less than 10% were obtained.

The simulations of the rod-rod arrangement are presented in Figure 13 and in **Papers VI** and **VIII**. For this calculation, two different simulations were made: one with the variable streamer zone without taking into account the electrical charge that can accumulate on the grounded electrode (i.e., without checking the condition that the electric field is high enough to generate streamers on the grounded electrode, namely, that the electric field is ≥ 750 kV/m) and the other one taking into account the criterion for negative streamer inception.

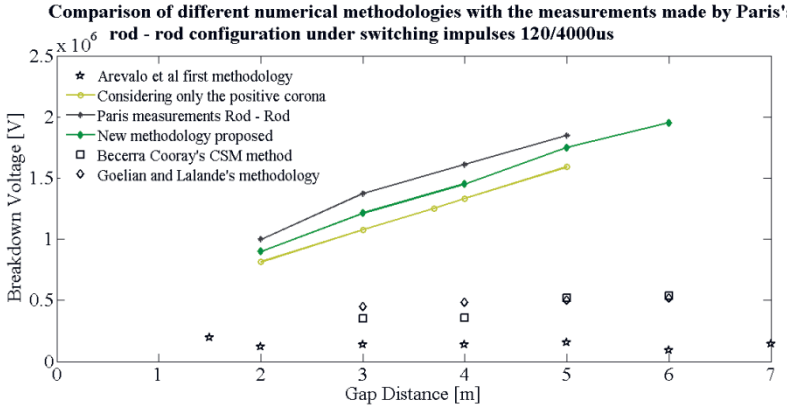

Figure 13. The 50% breakdown voltage for a rod-rod arrangement for different gap distances. Comparison between the models of Becerra and Cooray CSM [15], and Goelian and Lalande [13]; the model is introduced Section 3.1, and the method is described in this section.

The simulations revealed that calculations that assumed a constant streamer zone, such as those of section 3.1 [25], Goelian and Lalande [13], and Becerra and Cooray [15] will lead to incorrect breakdown magnitudes for a rod-rod gap configuration, with breakdown errors higher than 80% and values that are insensitive to changes in the gap distance. In contrast, when a variable streamer zone is used for the calculation without checking the streamer criterion on the grounded electrode, the errors in the breakdown voltages are still close to 20% when compared with the experimental results, however they follow the variation observed in the gap distance in the experimental measurements.

The results assuming a variable streamer zone, which took into account the streamer criteria in the grounded electrode, lead to an acceptable and con-

servative error of below 9%, for the distances evaluated and the variation found with the gap distance in the experimental measurements made by Paris [40, 41].

Thus, in the research presented in this part of the thesis, two changes have particularly improved the calculation of the propagation of the leader streamer in a long gap arrangement and the relevant research is discussed in depth in **Papers V** to **VIII**:

- A successful three-dimensional calculation of a variable streamer zone was proposed and implemented taking into account the minimum electric field that characterizes the propagation of the streamer region.
- The path of the discharge based on switching impulse measurements was incorporated in the methodology and different distributions were found to be required depending upon the electrode configuration under consideration.
- The calculation method results in errors of less than 10% and can be used in different gap configurations, such us rod-rod and rod-plane ones.

4 Validation of the methodology through ultra high voltage laboratory experiments

ABB Power Systems HVDC – Ludvika [46] performed several long gap experiments under positive switching applied voltages to investigate the insulating behavior of air at ultra high voltages. The series of experiments conducted consisted of using different electrode configurations with gap distances that were varied between 6 and 10 meters; and, to the gaps, switching impulse voltages were applied. The methodology developed and explained in Chapter 3 was utilized. The breakdown voltages and the time to breakdown were calculated and compared with the experimental results and very good accuracy was observed.

4.1 Experimental set-up

The experimental tests were performed at the Ultra High Voltage Laboratory UHVEN at ABB – Ludvika. The applied voltage consisted of positive switching impulses (250/2500 s). Two electrode arrangements were used: rod-plane and sphere-plane. The gap distances were varied from 6 to 10 meters; and the insulation media in all the tests was air under normal atmospheric conditions. The humidity and temperature were registered. The up and down method was used to test the different configurations following the IEC standards [47]. For each voltage level, 30 shots were applied. The breakdown voltage and the time to breakdown were measured.

Two cameras were installed at 90 degree angles to enable them to photograph the path of the discharge in 3D-planes, and for every shot two photographs were recorded. A fast video camera was used as well to register the speed of the leader propagation and the geometry of the path of the discharge.

4.1.1 Rod-plane air gaps

The rod used was a 6 meter long metallic rod terminated at the top by a fine electrode with a grounded metallic plane located on the floor. The distance to the wall was chosen in such a way that there was no probability of breakdown occurring against the wall for any of the experiments performed. The gap distance was varied between 6 and 10 meters. The high voltage source was directly connected to the rod electrode and the plane was well grounded.

A total of 30 impulses was applied to every gap arrangement and the voltage measurements were registered as a function of time until the breakdown had occurred. The breakdown voltage and the time to breakdown were simulated for each of these individual breakdowns and the values obtained were compared with the experimental values. Figure 14, illustrates the path the discharge took in a gap distance of 6 meters for a rod-plane configuration; the sequence of figures was taken with the fast video camera, as the discharge steps along the path.

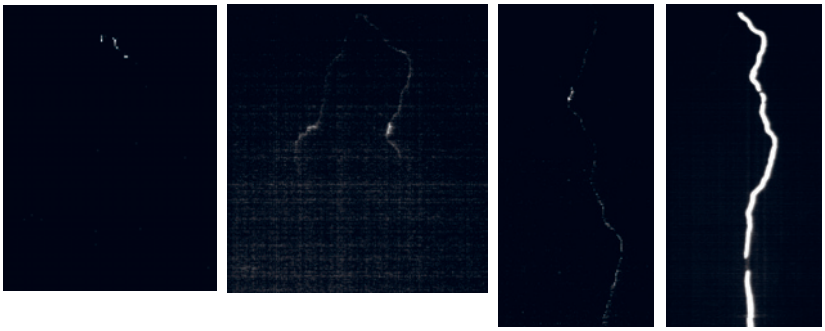

Figure 14. Sequence of the path of a discharge in a 10 meter gap obtained after processing the video taken during the discharge. (a) the discharge at the initial time, 10 μs, (b) after 40 μs, (c) after 120 μs and (d) at 180 μs.

As explained in Section 3.2.1.2., the constants a_1, b_1 and c_1 are required for the calculation of the tortuous path of the discharge; the Gaussian distribution and its respective constants are obtained from fitting the photographic evidence for each impulse applied to the 6 to 10 m long spark gaps. Table 3 presents the different magnitudes for the different kinds of rods used on the high voltage electrode.

Table 3. Coefficients of the tortuous Gaussian distribution with 95% confidence limits.

Constant	Square rod
a_1	3.65 (3.11, 4.0)
b_1	0.051(-0.07, 0.17)
c_1	0.28 (0.16,0.41)

Using the Gaussian distribution presented earlier and the characteristics of the set-up, each applied switching impulse voltage was simulated and the results are summarized in the following tables. The error between the simulation and measurements is displayed as well.

Measurements					Simulations			
Applied Voltage [kV]	Breakdown Voltage [kV]	σ	Time to breakdown [μs]	σ	Breakdown Voltage [kV]	Time to breakdown [μs]	% error in V_b	% error in t_b
1500	1464,8	2,39	287,81	18,43	1494,6	287,7	-2,03	0,04
1560	1523,5	3,53	339,13	26,09	1548,9	280,43	-1,67	17,31
1440	1409,83	1,72	290,23	14,52	1429	306,15	-1,36	-5,48
1380	1353		330,63		1342,2	391,6	0,80	-18,44

Table 4. Simulations and measurements of the breakdown voltage and the time of the breakdown with the percentage error for a rod-plane arrangement for a gap distance of 6 meters.

Measurements					Simulations			
Applied Voltage [kV]	Breakdown Voltage [kV]	σ	Time to breakdown [μs]	σ	Breakdown Voltage [kV]	Time to breakdown [μs]	% error in V_b	% error in t_b
2160	2099,5	7,61	541,15	124,6	2158,15	479,17	-2,79	11,45
2070	2026,4	5,98	536,48	76,47	2026,3	467,31	0,01	12,89
1980	1937	2,64	524,1647	45,19	1948,7	425,35	-0,60	18,85

Table 5. Breakdown voltage and time to breakdown obtained in simulations and measurements with the percentage error for a rod-plane arrangement with a gap distance of 10 meters.

The results of the simulations have shown that the methodology can reproduce the experimental results obtained for the rod-plane configuration with good accuracy. The maximum error obtained was 3% for the breakdown

voltage and the average error in the calculation of the breakdown voltage was 1.13%. The maximum error determined in the calculation of the time to breakdown for a single test was 19% and the average obtained error was 14.4%.

4.1.2 Sphere-plane configuration

The second set-up used for the comparisons was an arrangement comprised of a sphere connected at the high voltage electrode and the grounded plane electrode. Two different spheres of 1.3 and 1.6 m radii were tested, and the gap distance between the sphere and the grounded electrode was varied between 4, 6 and 8 m. As in the previous test, 30 impulses were applied using the up and down method. The test was implemented with the photographic equipment described above. The data obtained were used to determine the Gaussian distribution of tortuosity for the sphere-plane arrangement.

For the simulation, every case was analyzed individually and the coefficients obtained for the Gaussian distribution are presented in the following table.

Table 6. Coefficients of the tortuous Gaussian distribution with 95% confidence limits.

Constant	Sphere
a_1	2.30 (0.68, 3.97)
b_1	0.88 (-0.40, 2.17)
c_1	1.13 (-0.42, 2.65)

The data obtained from the measurements are summarized in tables 7, 8 and 9. The percentage error is compared for the breakdown voltages and the time to breakdown.

Measurements					Simulations			
Applied Voltage [kV]	Breakdown Voltage [kV]	σ	Time to breakdown [μs]	σ	Break-down Voltage [kV]	Time to breakdown [μs]	% error in V_b	% error in t_b
2150	2148		680,57		2063,7	439,32	3,924	35,44
2240	2175,79	5,3	352,38	20,1	2076,5	318,6	4,563	9,58

Table 7. The breakdown voltage and the time to breakdown obtained from simulations and measurements, with the percentage error, for a sphere of 1.3 m diameter in a sphere-plane arrangement with a gap distance of 6 m.

Measurements					Simulations			
Applied Voltage [kV]	Break-down Voltage [kV]	σ	Time to break-down [μs]	σ	Breakdown Voltage [kV]	Time to break-down [μs]	% error V_b	% error t_b
2400	2326,7	6,26	427,05	36,98	2146,4	404,32	7,75	5,32
2320	2300,5	4,14	521,8	37,5	2135	415,32	7,19	20,41
2240	2207		361,65		2135,5	334,39	3,24	7,54

Table 8. The breakdown voltage and the time to breakdown obtained from simulations and measurements, with the percentage error, for a sphere of 1.3 m diameter in a sphere-plane arrangement with a gap distance of 8 m.

Measurements					Simulations			
Applied Voltage [kV]	Break-down Voltage [kV]	σ	Time to break-down [us]	σ	Breakdown Voltage [kV]	Time to break-down [us]	% error V_b	% error t_b
2440	2332	7,25	196,166	4,54	2202,6	177,61	5,55	9,46
2360	2337	8,8	264,3	28,17	2195,6	220,32	6,05	16,64

Table 9. The breakdown voltage and the time to breakdown obtained from simulations and measurements, with the percentage error for a sphere of 1.3 m diameter in a sphere-plane arrangement with a gap distance of 4 m.

From the results of the simulation is possible to conclude that the simulations can reproduce the experiment with very good agreement. The maximum error for the breakdown voltage is 7.75% and the average error is 5.36%. The time to breakdown presented higher errors than the breakdown voltage; the maximum error in the time was 20.41%, obtained for the gap distance of 8 meters and the average error for all the tests was 15.6%. It is important to note that the simulated magnitudes of the breakdown voltage are lower than the measured values, which will give a conservative value from the point of view of designing the insulation.

4.1.3 Variable distance to the wall

With the aim of evaluating the precision of the simulation when the background electric field changes because of the presence of a wall (another grounded electrode) and when two gaps are competing (wall-high voltage electrode, high voltage electrode-wall), simulations were made of a sphere-plane gap with a variable distance to the wall. Simulations of breakdown to the wall and breakdown to the grounded plane were evaluated independent-

ly. The experimental measurements were carried out at ABB Ludvika [48], and the experimental set-up consisted of a 1.3 m diameter sphere and a grounded metallic plane. Four different gap distances to the earthed electrode were tested and four distances to the wall. As in the previous series of experiments, for every test, 30 switching impulses were applied and every single test was simulated. The magnitudes of the breakdown voltage and current were calculated and the results, with their respective errors, are summarized in the following table.

Gap m	Dist. to Wall	Breakdown Voltage 50%		% error	Time Breakdown 50%		% error
		Measurement	Simulation		Measurement	Simulation	
4	6	1825	1649.7	9.61	193.8	192	0.93
4	10	1869	1829	2.14	195.4	193.6	0.92
5	10	1962	1816	7.44	248.9	224.7	9.72
6	10	2025	1821	10.07	314.6	296.3	5.82
8	10	2125	2096	1.36	375.1	369.9	1.39
6	8	1965	1921	2.24	337.3	319	5.43
5	8	1918	1800.9	6.11	263.1	204	22.46
6	7	1937	1805.3	6.80	373	314.3	15.74
5	7	1918	1878.9	2.04	263.1	257.6	2.09

Table 10. The measured and simulated breakdown voltage and time to breakdown, with the error calculation for a sphere-plane configuration. The diameter of the sphere was 1.3 m for all the cases and the gap distance and the distance to the wall were varied.

As is evident from table 10, the maximum error in the breakdown voltage was 10% and the average error was 5.31%. For the time to breakdown, the error was higher than the error in the breakdown voltage; the maximum value was 22.46% and the average magnitude was 7.16%.

These results show that the methodology can reproduce the breakdown voltages and the times to breakdown more accurately by taking into account the effect of changes in the background electric field. It is important to mention that the magnitudes of the breakdown voltage for sphere-plane gaps are conservative from the point of view of determining the insulation requirements (i.e., lower magnitudes are obtained for the breakdown voltages using the proposed methodology than those found in the measurements).

From this chapter it is possible to conclude that:

- The results showed that the methodology proposed in **Chapter 3** can reproduce the breakdown voltages and the times to breakdown for the sphere-plane and rod-plane configurations with good accuracy. The average error for the breakdown voltage is lower than 6% and for the time to breakdown is lower than 22% in the worst case.
- The effects of nearby walls, which will change the background electric field, are successfully reproduced using the proposed methodology.
- The methodology was tested with several experimental measurements and it was observed that the magnitudes of the breakdown voltages calculated are lower than the measurements. This gives a conservative value that can be used to design protection distances.

5 Negative leader discharges under switching impulses

The majority of the modeling work has been dedicated to the consideration of positive discharges because of the complexity of the negative discharge process. In nature, however, most of the lightning discharges are of negative polarity. Therefore, the development of numerical models capable of reproducing negative discharges will improve the design of lightning protection systems and the design of equipment that can withstand overvoltages caused by direct and/or indirect strikes.

A first step to attaining the goal of modeling negative lightning discharges is to model laboratory gap discharges, as these are developed in controlled environment; for example in the form of laboratory discharges under switching impulses, as presented in **Papers IX** and **X**.

5.1 Mechanism behind negative leader discharges

The physical description assumed here is based on the characteristics presented by Castellani 1998 [49], Les Renardieres 1978 [4], Lalande 2002 [50] and Gallimberti et al 2002 [17]. This description corresponds to observations of experiments conducted with a rod-plane arrangement to avoid interaction between positive and negative discharges.

The first phenomenon that occurs during a negative discharge is the formation of a negative streamer (NC) at time t_i. Then afterwards, at time t_1, a discharge process called a "pilot" appears (PL), in which simultaneous development of a positive streamer propagating towards the cathode and a negative streamer propagating towards the anode occurs.

At time t_2, a space leader (SL) develops from a space stem, and at t_3, the conditions are ripe for a negative leader (NL) to propagate towards the anode. From the published results [11, 17], one can conclude that the thermodynamic conditions for the formation of positive leaders ought to be very similar to those for negative leaders.

At time t_4, a stem is formed in the space where the two pilots were located. However, this stage is not observed for gaps of less than 4 m [4, 49]. From this stem, a negative streamer and a leader crossing the space (SL) are formed. The leader possesses two heads, one of which is a positive leader and propagates towards the cathode, the other, being a negative leader, propagates towards the anode.

When the space leader reaches the negative electrode, a negative streamer is formed and the leader channel is illuminated brightly. This step is called a step discharge. Briefly, the negative discharge propagates discontinuously, hence the name, and with complex processes taking place between the negative and positive streamers. Figure 15 was taken from [17] to illustrate the various stages of a negative discharge.

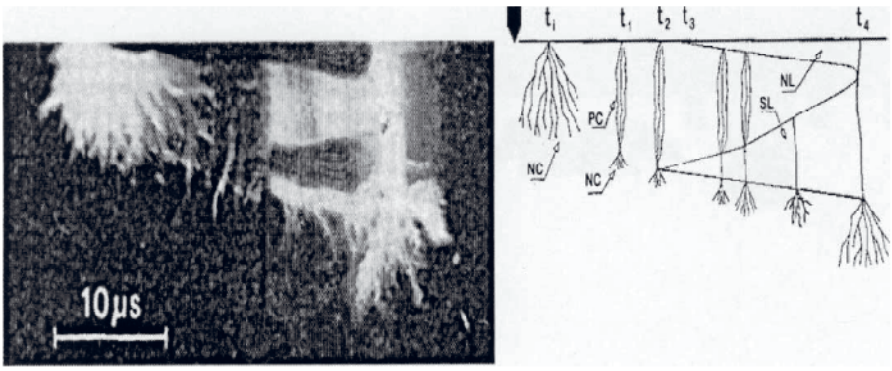

Figure 15. Negative leader development process. This figure has been reproduced from [17] with the permission of Elsevier.

5.2 Negative leader models

The first lightning attachment model incorporating physical assessments was proposed by Dellera and Garbagnati [51]. This model, called the leader progression model, includes the simulation of the propagation of both negative and positive leaders using electrostatic considerations. Subsequently, from Les Renardieres' experimental work [1, 3], Gallimberti [10] developed the physics pertinent to understanding the development of leaders. Subsequently, Gallimberti and Bondiou [11] built up a physical methodology that simulates positive upward leaders under switching impulses. Taking the work of Bondiou and Gallimberti [11] as their starting point, Becerra and Cooray developed a model to study the attachment of lightning flashes to grounded structures[15]. However, neither Dellera and Garbagnati [51] and Rizk [8,

7], nor Becerra and Cooray [15] modeled the negative steeped leader from first principles.

In 1994, Bacchiega et al [52] developed the first theoretical model of the propagation of a negative stepped leader across long air gaps. By 1998, Castellani et al [49] had conducted experimental measurements in such long gaps to identify the bi-leader process, giving a great amount of detail of the negative leader development.

In 2000, Mazur et al [53] presented the results of a physical model of negative leaders generated under the effect of a downward-coming positive leader. In 2002, Gallimberti and Lalande et al [17, 50] presented a bipolar model to reproduce triggered lightning in which they included positive and negative leaders based on the measurements of Les Renardieres [3] and Castellani [49] and the model of Bacchiega [52].

The other available models are stochastic, such us the electrical breakdown models of Niemeyer et al. [54], Tsonis and Elsnet [55], and Sanudo et al. [56], with some of them using the electrical characteristics of the leader channel published by Petrova [57]. The latest available model by Beroual et al [58, 59] takes electrical network parameters derived from electromagnetism, wave propagation and gas discharge theory to calculate the evolution of a lightning discharge.

All of the above-mentioned models are approximations that fail to reproduce all the different stages of the negative discharge in one way or other. Therefore, to reproduce processes such as the relaxation time or the positive leader propagation or space leader, they tune parameters or assume circuital arrangements.

5.3 A preliminary model to simulate negative leader discharges under switching impulses

In **Papers IX** and **X**, a new physical model is proposed that takes into account the stages and characteristic measurements identified by Castellani [49] and the subsequent phases of the physics of the negative discharge identified and used by Castellani, Mazur and their co-workers [49, 50, 53]. The methodology considers processes such as the negative leader channel, composed of a negative and positive streamer and the negative leader stem. For the positive and negative streamer, we used the streamer criterion of Gallimberti [10].

Once the first streamer has been incepted, the charge in the streamer zone is calculated, assuming that the streamer zone is characterized by a constant electric field of 450 kV/m and 750 kV/m for positive and negative streamers, respectively. The next stage is the so-called "pilot system", and the calculation is made as described in **Paper X**.

The voltage drop in the leader channel was evaluated using the LTE equations of Gallimberti [10]. The step leader propagation is reproduced until the final jump takes place. The condition for the final jump is satisfied when the negative streamer reaches the grounded electrode. Figure 16 presents the flow diagram for the calculation.

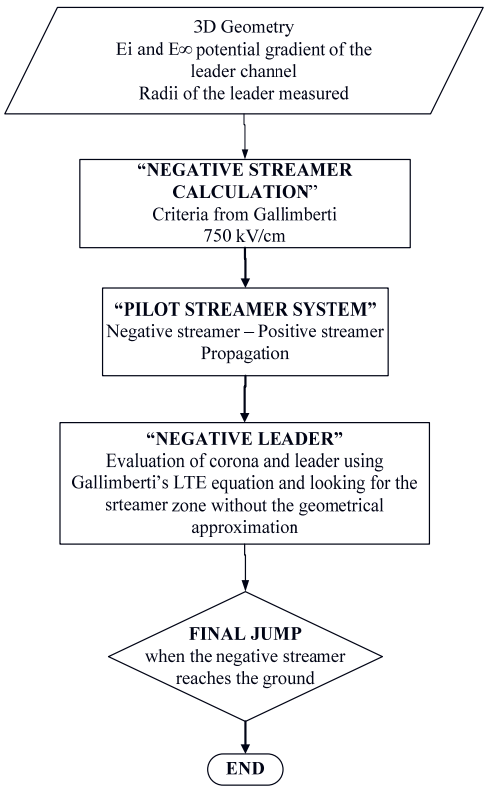

Figure 16. Flow chart for the simulation of the development of the negative leader. E_i is the electric field at the start of the leader and E_∞ is the electric field at infinity attributable to the leader channel

5.3.1 "Pilot streamer system"

Even though there is no clear explanation of the physics underlying the discharge process because of its complexity and the lack of experimental data, some experimental results have indicated that each pilot streamer discharge starts at the lower tip of the preceding one and that this form of initiation is associated with every current pulse [4, 49]. A consistent explanation has, however, been proposed by Bacchiega and co-workers [52].

For the calculation of the potential profile and the reproduction of a pilot system, the following considerations have to be taken into account:

1. It has been stated in the literature that the electric field necessary for the propagation of a negative streamer is constant and has a value of 750 kV/m [10]. Therefore, the region in front of the tip that fulfills this electric field criterion has been identified, and the maximum axial length of the region has been calculated.
2. Once the negative streamer is formed, a positive leader discharge will develop in the direction of the high voltage electrode. The simulation of this positive leader follows the methodology presented in Chapters 3 and 4. The inception and direction of the propagation of this positive leader is assumed to be at the central axis of the arrangement towards the high voltage electrode.
3. Laboratory measurements made by Les Renardieres' Group have shown that, before the formation of the first pilot system, there is an enhancement of the electric field between the negative streamer and the grounded electrode, leading the electric field in the local region next to the tip of the negative streamer to have a magnitude of $1 \cdot 10^6$ V/m [4]. The existence of this electric field in the vicinity of the tip of the negative streamer region and the requirement that a positive discharge can propagate towards the high voltage electrode makes it necessary to assume that, from the tip of the negative streamer region, a first stem leader develops towards the high voltage electrode with an electric field magnitude of $1 \cdot 10^6$ V/m. In front of this stem leader, a positive streamer is located.
4. For the simulation of the positive and negative leader channel Gallimberti's LTE equation is used [10].
5. The potential distribution of every pilot streamer discharge will be composed of the potential drop: over the positive streamer region, in the positive leader channel and in the negative streamer region located in front of the grounded electrode.

There are plenty of different phenomena going on that need to be

considered, these effects are: the positive leader channel, the positive and the negative streamers, and when they are combined, the relative impact of the different phenomena gives the total charge, which leads to the characteristic pulsing of the pilot system, defined by the so-called "relaxation time", which has been tuned to RLC electrical circuits in other models.

The charge per unit length that is necessary to sustain the progression of the pilot streamer discharge was assumed to be 13.8 μC/m as this was the value measured by Castellani and co-workers [49]. In Figure 17, one can observe the potential profile distribution before and after the streamer development, and after the formation of the first pilot streamer discharge.

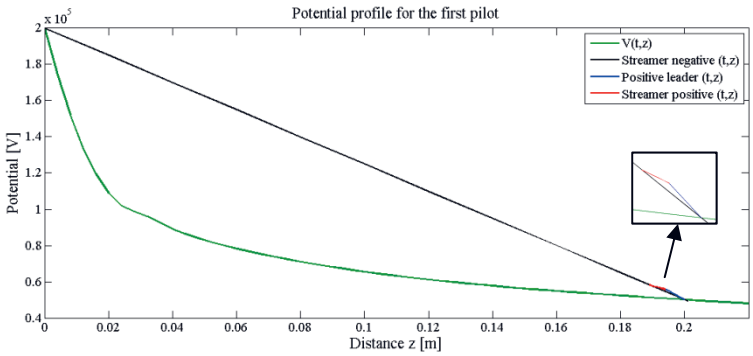

Figure 17. Potential distribution before and after the negative streamer development and after the formation of the first pilot streamer discharge. The insert shows an enlargement of the potential of the incepted leader and the streamer channel.

5.3.2 "Negative leader phase"

The measured results extracted from the literature [4, 49] reveal that the charge required to incept a leader channel is of the order of 5.4 μC. This value was used in the present calculation to initiate the simulation of the leader stage. This charge includes all of the charge associated with the different streamers and the pilot systems developed up to the inception of the leader.

We assumed that the inception mechanism for the negative leader is similar to the one for the positive leader [60]. This is reasonable because the threshold charge corresponds to the charge necessary to heat the "stem" to a critical temperature, which will lead to the formation of the first section of the leader channel. To calculate this negative leader, the thermo-equilibrium

equations of Gallimberti [10], described in Chapter 2, are used. The initial condition of the potential gradient before a new leader segment is created is assumed to be 7.5 x 10^5 V/m, taken from experimental evidence [10], which is a different condition from the one assumed for positive leaders. The charge per unit length necessary to sustain the negative leader propagation used in the simulations was 108 μC/m based on values published in the literature [49].

5.4 Application of the methodology

In order to check the validity of the model, two different rod-plane configurations were tested, with two different switching impulses and gap distances. The results are presented in **Paper X**. First, the methodology was applied to the same geometrical set-up as that used by the Les Renardieres Group [3], which consists of a gap between a conical rod and a plane. The conical electrode had a tip radius of 10 mm. The simulation was made assuming a gap distance of 2 m with an applied voltage of -1550 kV; a waveshape of 20/1600 μs was used.

The results of the simulations presented in Figures 18 and 19 showed that the trend exhibited by the simulated current agrees with the measured signatures determined by the Les Renardieres' Group. The maximum magnitude of the current is 10 A for both the measurements and simulations. The simulation of the current pulsates, which is because of the restarting process and because of the exchange of charge in the channel arising from the presence of both a negative leader and a positive leader moving towards the high voltage electrode.

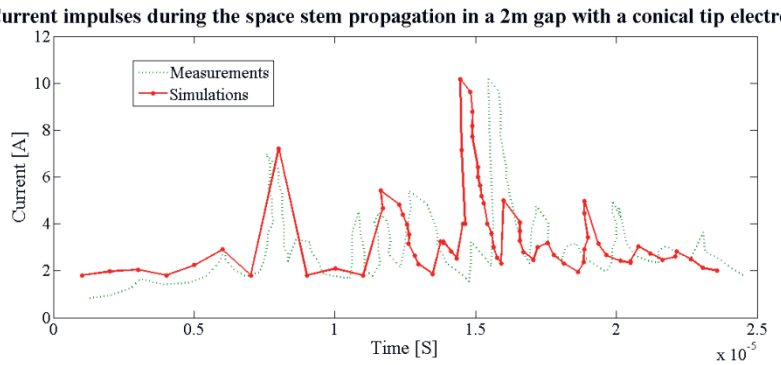

Figure 18. Measured and simulated current pulses during the stem-space propagation in a 2 m wide gap between a conical rod and a plane with a switching impulse of 20/1600 μs, configuration used by Les Renardieres.

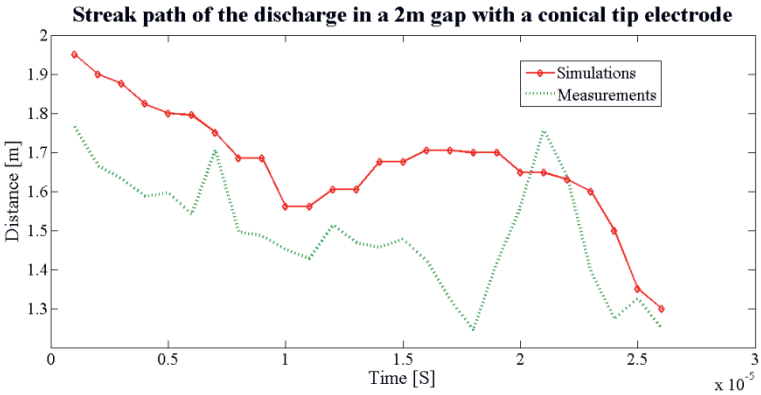

Figure 19. Results of simulations obtained using the measurements of Les Renardieres for a 2 m conical rod-plane gap during a switching impulse of 20/1600 μs.

Overall, the model results including the path of the discharge are in good agreement with the experimental results of Les Renardieres [3]. However, it is important to notice that, even though the shape of the pulses is in agreement with the measurements, slight differences are evident in the timing. All pulsation behavior corresponds to the pilot streamer system representation and that the initiation of pilot streamers is dependent on the exchange of positive and negative charges.

The final parameters available for comparison are the time to breakdown and the breakdown voltage, which were calculated and are summarized in Table 11.

	Breakdown Voltage [kV]	Time to Breakdown [μs]
Les Renardieres	**1481**	**20.6**
Simulations	**1546**	**28**
% error	**4.5**	**35.9**

Table 11. Comparison between the measurements and the results of the simulations for a 20/1600 μs impulse across a gap of 2 m between a conical rod and a plane.

The time to breakdown and the breakdown voltages exhibited errors of 35.9% and 4.5%, respectively, for the particular case shown. The higher error in the time to breakdown can be attributed to the path that the discharge has taken. As was demonstrated in the references [60, 61], the path followed by the discharge determines the time to the breakdown, but it does not have a notable influence on the calculation of the breakdown voltage.

Owing to a lack of detailed experimental information in the literature, it is not possible to extract more parameters for the same configuration, but data

for positive and negative streamer charges and for the velocity of the positive and negative leaders can be obtained from the calculation. A comparison with a gap distance of 7 m, maximum voltage 2.8 MV and a waveform of 6/3000 μs using the configuration studied by Les Renardieres [4] was made and the results can be found in **Paper X**.

A self-consistent numerical simulation based on the physical process behind the negative leader discharge has been presented in **Papers IX** and **X**. It includes a novel way to calculate the streamers for the pilot system and enables the complete negative discharge to be predicted. The experimental results are compared with simulations and show good agreement on the representation of the magnitudes of the current and path of the discharge.

6 The lightning attachment process and applications to IEC standards

The theories and the design of the protection of structures against lightning rely heavily on the data for long gap discharges. The methods accepted as the standards were derived from empirical approximations or equations taken from data from long gap experiments under switching impulses. Various authors from the scientific community have proposed models that adopt a more physical approach to the representation of the lightning attachment process. Nevertheless, some assumptions concerning the initial values or regarding the nature of the process have had to be made.

6.1 Lightning protection models and standards

Lightning protection standards laid down by the IEC [62, 63] specify three procedures that can be used to implement a lightning protection system for grounded structures. They are the rolling sphere, the mesh and the protection angle methods.

The rolling sphere method comes from a simplified version of the electro-geometric method [64-67]. According to the electro-geometric method, a down-coming stepped leader will get attached to the first part of a grounded structure that comes within a critical distance of the tip of the stepped leader. This critical distance is called the *striking distance,* and was defined by Golde [19].

In the rolling sphere method, the radius of the sphere is selected such that its radius is equal to the striking distance. The radius of the sphere R is defined as a function of the probable return stroke current according to the relationship between the lightning striking distance and the peak return stroke current derived by Whitehead for power transmission lines [67]. The design of the lightning protection system uses the rolling sphere method, in which a sphere with a specified radius is rolled over the surface of the ground and over the structure to be protected, allowing the protected and the unprotected objects or parts of the structure, covered by the shadow of the sphere or

touched by the sphere respectively to be visualised [62, 67]. Any part of the structure that is in contact with the surface of the sphere is considered to be vulnerable to a direct lightning strike; the untouched volume falling outside the shadow of the sphere defines a lightning protected zone. The radius of the sphere is defined as being equal to 15 m or 50 m, depending upon the level of lightning protection required.

The second method proposed for the positioning of air terminals is the *protective angle method*. This procedure is recommended for simple structures. The positioning of air terminals, masts and wires is determined by taking into account the fact that all parts of the structure to be protected fall inside the volume defined by the surface generated by projecting a line from the air terminal to the ground plane, at an angle α to the vertical.

The equation defining the protective angle was established by Wagner *et al.* [68, 69]. The relationship between the connection distance for the upward and downward leaders, called the *final jump*, and the point at which the return stroke current I_p starts was proposed to be:

$$S = A \cdot I_p^b \,[\mathrm{m}] \qquad (6.1)$$

S is the final jump distance in meters, I_p is the peak lightning current in kA, and A and b are constants that take on different values depending upon the author [65, 66, 70-75]. Fixed angles are still in use as a design tool today.

The third method, especially recommended for the protection of flat surfaces, is the *mesh method*. According to this method, a conducting mesh is used with a cell size determined by the minimum return stroke current that is allowed to strike the protected structure [62]. The mesh has to be located at a critical distance above the flat surface to be protected to avoid a direct strike.

6.2 Lightning attachment model

A number of authors [12, 76, 77] have used lightning attachment models with the aim of probing the lightning protection methods accepted by the standards [12, 76, 77]. However, their results are not conclusive owing to the parameters assumed and/or the complexity of the routines applied. Thus, more results are needed to validate the methods accepted in the international standards.

The methodology used for long gap simulations discussed in Chapter 3 was extended and applied to the lightning attachment cases in an attempt to create a more physical approximation to the international standards and to improve the practical design of protection against lightning. A brief description of the methodology applied is presented here, a more detailed discussion can be found in **Papers XI-XIV**.

6.2.1 The methodology

The procedure adopted in the calculation is divided into three different stages. In the first stage, the structure is scanned to identify the locations at which the streamer inception criterion of Gallimberti [11] is satisfied. The second stage involves an analysis of stable leader inception. After the streamer inception criterion is fulfilled, the dynamic leader inception procedure is used to locate the points from which a stable leader can be incepted. The final stage involves the analysis of the movement of the upward leader towards the down-coming leader and the final attachment process.

6.2.1.1 **Streamer Criteria**

The methodology applied considers a straight downward-coming leader approaching a structure, as was first proposed by the leader progression model of Dellera and Garbagnati [27, 28] and later applied by Lalande [12] and Becerra and Cooray [15, 37, 76-77]. It consists of representing the downward leader as a line with a given charge density. The charge density is a function of the probable return stroke peak current and, in this case, its value is calculated using the equation proposed by Cooray et al [78]:

$$\rho(z) = 8 \cdot 10^{-6} \cdot \left(1 - \frac{\xi}{H - z_0}\right) \cdot G(z_0) \cdot I_p + \frac{a + b \cdot \xi}{1 + c \cdot \xi + d \cdot \xi^2} \cdot H(z_0) \cdot I_p \ \ [\mathrm{C/m}] \tag{6.2}$$

with

$$G(z_0) = 1 - \left(\frac{z_0}{H}\right)$$
$$H(z_0) = 0.3 \cdot e^{-\frac{z_0}{50}} + 0.7 \cdot e^{-\frac{z_0}{2500}} \tag{6.3}$$
$$\xi = z - z_0$$

where z_0 is the height of the leader tip above the ground in meters, H is the height of the cloud in meters (which is assumed to be equal to 4000 m), Ip is the peak return stroke current, $a = 7.2 \cdot 10^{-5}$, $b = 5.297 \cdot 10^{-5}$, $c = 1.316$ and $d = 1.492 \cdot 10^{-2}$.

The downward leader channel is divided into segments of increasing length from the base of the cloud to the tip of the leader to compute the background electric field. The charge density in each segment is assumed to be constant and is equal to the charge in the lower part of the segment as given by equation (6.2).

Once the first corona has been incepted, the charge in the streamer zone is calculated using the simplified electrostatic approach proposed by Lalande [12] and N. Goellian *et al* [13], which assumes that the streamer zone is characterized by a constant electric field. If the streamer inception criterion is fulfilled in one of the corners of the building, the leader inception procedure will be initiated.

6.2.1.2 **Leader Inception**

The stable leader inception criterion is divided in two parts: one involves the calculation of the charge and the dimensions of the streamer zone, and the other concerns the development of the leader channel. For the calculation of the features of the streamer zone, the procedure used by Lalande and Goelian et al [12, 13] is applied. This procedure assumes the streamer zone to have a fixed geometry with the number of streamers determined by the experimental measurements of Les Renardieres' Group [3]. However, the geometrical constant, K, for the calculation of the streamer zone proposed by Becerra and Cooray [37] was used in the analysis presented in **Paper XII**. The voltage drop in the leader channel was evaluated using the LTE equations of Gallimberti [10]. Once the radius of the leader channel was given as an input parameter, these equations predict the development of the electric field inside the leader channel.

For each time step, the potential caused by the leader channel and the potential change arising from the streamer zone were analyzed. The charge inside the streamer region was recalculated and was kept for the next time step, as was done by Lalande [12] and Becerra and Cooray [15]. Nevertheless, it is important to emphasize that the advance of the leader is not only calculated from the charge in the streamer zone, but also from the charge attributable to the leader channel. In addition, in the calculation presented here, no linear approximation was made for the background potential as had to be assumed in previous models [15, 76, 77].

6.2.1.3 **Lightning attachment**

Once an upward leader is incepted, it propagates in the direction of the downward-coming stepped leader. The simulated lightning attachment procedure consists of analyzing the propagation of the stable upward leader while the down-coming leader is approaching, as was done in the Becerra and Cooray methodology [37]. The calculation was terminated when the streamer zone of the upward leader reaches the downward-coming leader.

6.2.2 Applications to the lightning attachment process

The lightning attachment methodology was used to validate two well-known engineering concepts, namely the protection angle cone and the mesh method, which correspond to the respective topics of **Papers XI** and **XII**.

6.2.2.1 **The protection cone method**

Shielding wires are required to protect power lines against external overvoltages, such as lightning discharges. The basic idea of a shielding wire is to create a volume for the conductors of the power line that is protected, and which will offer effective protection against lightning strikes, in accordance with the standards. The angle of protection for the shielding wire can be determined using "the effective electro-geometrical method" [74, 75] or the "perfect shielding concept" [30, 66] if the magnitude of the current, and the heights of the conductor h_f and the shielding wire h_g are known. Figure 20 illustrates how the calculation of the angle of protection is carried out.

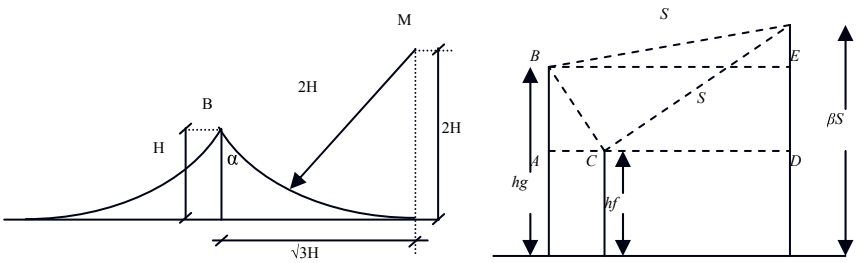

Figure 20. Determining the protection angle. The basic electro-geometrical method is illustrated on the left, where H is the height of the structure and α corresponds to the angle of protection. On the right, the perfect shielding concept is illustrated; *S* corresponds to the striking distance, *hg* to the height at which the shielding wire is located, and *hf* is the height of the conductor wire. β is a factor function of the return stroke current [79].

The calculation of the protection angle is based on the following equations:

$$
\begin{aligned}
k_1 &= \frac{h_g}{S} \\
k_2 &= \frac{h_f}{S} \\
\frac{x}{S} &= \sqrt{1-(\beta-K_1)^2} - \sqrt{1-(\beta-K_2)^2} \\
\alpha &= \arctan\left(\frac{x}{h_g - h_f}\right)
\end{aligned}
\tag{6.4}
$$

In the analysis, presented in **Paper XI**, four AC power transmission line structures were simulated, two for 230 kV and two for 500 kV. The position of the downward leader was changed in the *x*-*y* plane. Figure 21 depicts the variation of the position in the *y* coordinate for a transmission line of 230 kV. On average, sixteen different points were analyzed for each structure and each downward leader. The points considered correspond to the vertices of the structure, where the conductors and the shielding wire are supported, and, for each point on the structure an analysis was performed to determine whether there would be streamer or/and leader inception and/or leader propagation.

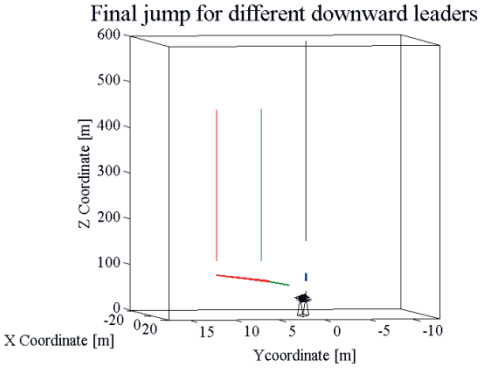

Figure 21. Position of the downward leaders and the distance between upward and downward leaders. The red line corresponds to the downward leader at *y = 10* [m], the green color corresponds to the downward leader at *y = 5* [m] and the black corresponds to the downward leader at *y = 0* [m].

The most important results are presented here, however the detailed results for every structure can be found in **Paper XI**. For a single circuit structure of 230 kV, the simulations showed that the shielding wire is always struck rather than the other wires. Even so, inception of streamers and leaders takes place on the other conductors. Table 12 includes a summary of the position

of the downward and upward leaders when the final jump condition is reached.

Downward leader		Downward leader conditions; *z*-coordinate [m] at the point analyzed				
		Shielding wires		Conductors		
x *[m]*	*y* *[m]*	*y*-coordinate = -3.96 m	*y*-coordinate = 3.96 m	*y*-coordinate = 0 m	*y*-coordinate = -7.92 m	*y*-coordinate = 7.92 m
0	0	42.31	42.31	27.25	35.25	35.25
0	5	43.18	45.01	27.32	33.32	33.95
0	10	38.42	40.48	23.33	31.33	31.41

Table 12. Final Jump: The results for different *y*-coordinates for the downward leader over a 230 kV single circuit structure. The z-coordinate at which the downward-coming leader is located when the final jump condition is reached is displayed for the shielding and the conductors.

For a double circuit structure, like the 500 kV one, the results showed that there is leader inception on the points where the conductors are supported, but there is no leader propagation from the points of inception.

Downward Leader Position		Downward leader z-position			
x [m]	*y* [m]	Shielding wire 40.36 [m]	*Phase A* 52 [m]	*Phase B* 37 [m]	Characteristic of upward leader for phases A and B
0	0	72.5 Final jump	69.39	65.22	Streamer inception
0	5	79.43 Final jump	69.29	70.22	Leader inception, not propagation
0	10	79.41 Final jump	69.28	66.43	Leader inception not propagation
0	15	83.43 Final jump	69.28	64.54	Leader inception not propagation

Table 13. The calculated z-coordinate corresponding to different stages of the discharge for the analyzed points on the structure.

The main conclusions of **Paper XI** are discussed below; the reader is referred to the publication for the other results.

If the downward leader goes inside the striking distance zone, connection will take place on the shielding wire, as is claimed by the electro-geometrical method [62, 63, 70, 71], and as was evident from the reported data of Brown and Whitehead [66].

The 230 kV single circuit structures have a double shielding protection wire. Nevertheless, from the points at which the conductors are supported, leader inception and propagation are possible. This result explains why some shielding failures have been reported for this type of structure [57]. In the double circuit configurations, upward leader inceptions at points other than the shielding wire are obtained, but there is no connection to them.

The cone of protection concept ensures that the area inside the cone is protected against lightning strikes and that the lightning will strike on the shielding wire before the protected region. However, the cone of protection does not prevent aborted connected leaders starting from the protected areas. Therefore, one can conclude that the cone of protection concept was validated for the simulated conditions and cases.

6.2.2.2 **The mesh method**

The aim of **Paper XII** was to review the effectiveness of the mesh size proposed in the standards by means of a procedure that takes into account the physics of the lightning attachment process.

The ideal protection procedure, according to the principles of electricity, is to enclose the protected object within a perfectly conducting shield of a thickness adequate to prevent it from melting. In practice however, it is not possible to perform such an ideal protection procedure, instead the structure is surrounded by a conducting mesh. The size of the mesh that should be used is specified in the standards [62, 63] and depends on the "Lightning Protection Level" required, the definition of which is based on the maximum amplitude of the return stroke current that the structure can accept without causing any damage either to the structure or to the contents of the structure. The mesh size is determined from the analysis conducted using the rolling sphere method. The separation between the mesh and the grounded structure should be larger than a critical value, and this critical value is also given in the standards and presented in Table 14.

Class of LPS	Mesh Size [m]	Minimum Current Standards [kA]	Critical height of mesh above the structure [m]
I	5 x 5	3	0.15
II	10 x 10	5	0.42
III	15 x 15	10	0.63
IV	20 x 20	15	0.84

Table 14. Magnitudes and levels of protection proposed in the standards IEC 62305 and the height of the mesh with respect to the ground level.

In the analysis, the total size of the analyzed plane is 100 x 100 m. The mesh was earthed and elevated above the ground level. The radius of the conductors of the mesh was assumed to be 2.5 mm as stipulated in the standards. In the analysis, the vertical axis of the stepped leader is located directly at the center of a cell, itself located at the center of the mesh. As the stepped leader approaches the grounded structure, the electric field at the mesh continues to increase and, when it reaches a critical value, a connecting leader is initiated from the mesh. In order to check whether the down-coming stepped leader will get attached to the connecting leader (i.e., the flash is intercepted by the mesh) or to the ground plane (i.e., the stepped leader penetrates the mesh) the following criteria are utilized: (a) If the streamers of the connecting leader approach the stepped leader to such a distance where the background electric field generated by the stepped leader is 500 kV/m, the criterion for the interception of the stepped leader by the connecting leader is assumed to have been satisfied. (b) If the electric field in the ground level just below the stepped leader reaches a value 10^6 V/m or more, after taking into account the screening by the mesh, it is assumed to have met the conditions for the stepped leader to terminate on the ground plane.

Condition (a) assumes that, once the positive streamers of the connecting leader reach the zone where the electric field generated by the stepped leader is larger than 500 kV/m, the streamers will propagate continuously until they meet the streamer sheath of the leader channel, thereby satisfy the final jump condition. The fulfillment of condition (b) assumes that the negative streamers of the stepped leader will reach the ground plane, and, thereby, they will meet the final jump condition between the stepped leader and the ground plane. Depending on which condition materializes first, the stepped leader will either get attached to the grid or to the ground plane.

The results from the simulations, displayed in Table 15, showed that the minimum values for the current specified in the standards pertinent to a given mesh size are in reasonable agreement with the results obtained in this study using a physically reasonable attachment model. The reason for this agreement is probably the fact that, in the case of a mesh located close to a ground plane, the leader has to come into the vicinity of the mesh before a connecting leader is issued by the mesh. This is so because a mesh placed rather close to the ground plane does not provide significant field enhancement to promote connecting leaders. As the length of the connecting leader diminishes, the attachment procedure becomes increasingly close to that simulated by the rolling sphere method, thereby bringing the results from both procedures closer to one another.

Class of LPS	Mesh Size [m]	Return stroke Current [kA]	Result
I	5x5	2	Attachment to ground
	5x5	3	Attachment to mesh
II	10x10	3	Attachment to ground
	10x10	4	Attachment to ground
	10x10	5	Conditions for attachment to the ground and to the grid are fulfilled almost at the same time
	10x10	6	Probable attachment to mesh
	10x10	7	Attachment to mesh
III	15x15	8	Attachment to ground
	15 x 15	9	Probable attachment to mesh
	15 x 15	10	Probable attachment to mesh
	15 x 15	11	Attachment to mesh
IV	20 x 20	13	Probable attachment to mesh
	20 x 20	14	Probable attachment to mesh
	20 x 20	15	Attachment to mesh

Table 15. Results of the simulations. If the electric field at the ground plane is less that 10^6 V/m, but greater than $7.5x10^5$ V/m when the criterion for the attachment of the leader to the mesh is satisfied, the outcome is denoted as probable attachment to the mesh. In the simulations, the height of the mesh above the ground plane is 0.2 m, 0.5 m, 0.7 m and 0.9 m for LPS classes I, II, III and IV respectively.

6.3 Multiple connecting leaders from a grounded structure

Simulations can be achieved by making assumptions, or by simplifying the representation of the physical processes. In the simulations of lightning attachment, one can approximate parameters such as the magnitude of the minimum or maximum electric field, leader velocities, the electrical charge required for leader inception, and the geometrical shape of the streamer zone, among others. However, if one supposes that most of the parameters assumed are correct, there is still another event that is potentially involved in the phenomena of lightning attachment that has not been taken into account in previous models [12, 37], which is the simultaneous inception of several upward leaders.

The fact is that, when a downward moving leader approaches a given structure, several connecting leaders could be initiated from several locations on the same structure. This is the case since, when immersed in the

background electric field of the down-coming leader, the electric field at several points on the structure may exceed the critical values necessary for leader inception. Consequently, two or more upward leaders can be generated and propagated from the structure. The initiation and propagation of several upward leaders from the structure would completely change the electric field configuration in the vicinity of the structure. This, in turn, would affect the propagation characteristics of the upward leaders and hence the lightning attachment process. None of the studies identified in the literature has analysed the effect of these multiple leaders on the lightning attachment process. Thus, in **Paper XIII,** a first approximation of the effect that two upward leaders being emitted at the same time would have on the lightning attachment process was presented, in which the simulated cases assume symmetry for the downward-coming leader. With the aim of introducing a more realistic condition, an assymetric position of the downward- coming leader is analyzed in **Paper XIV**.

For both papers, the applied methodology considers a leader coming straight down over a structure, as described in Section 6.2.1.1. The structures envisaged were rectangular buildings, and details of their dimensions can be obtained in the respective papers.

The results pertinent to both papers showed that the propagation characteristics of the upward connecting leader are influenced by the presence of other leaders. They very clearly demonstrate that the moment one connecting leader starts accelerating towards the downward-coming stepped leader, the growth of other connecting leaders is arrested. The reason for this is that the charge deposited in space by the accelerating connecting leader reduces the electric field in the vicinity of other connecting leaders, thereby impeding their motion. It is also observed that a slight advantage from the background electric field is enough for one connecting leader to take over, forcing the others to abort the attachment process.

The calculations performed in **Paper XIV** showed the current and velocity of two upward leaders generated from grounded rods; the location of the downward-coming leader is asymmetric to the rods, being closer to the rod denoted by the letter A than to the one called B. Figure 22 displays the current associated with the connecting leaders from rods A and B and depicts the speed of the connecting leaders. Note that the current in the connecting leader from A grows monotonically until the final jump condition is satisfied, whereas the current from B increases initially, but then drops off to zero as the leader from rod A takes over. A similar tendency can also be seen in the case of the leaders' speeds. As one can appreciate that, after several unsuccessful attempts (unstable leader inception), the two leaders would start

off with similar speeds. However, as the stepped leader comes closer to the structure, the leader from A starts to grow very rapidly. In coincidence with this, the growth of the connecting leader from B is arrested, and it is aborted almost immediately.

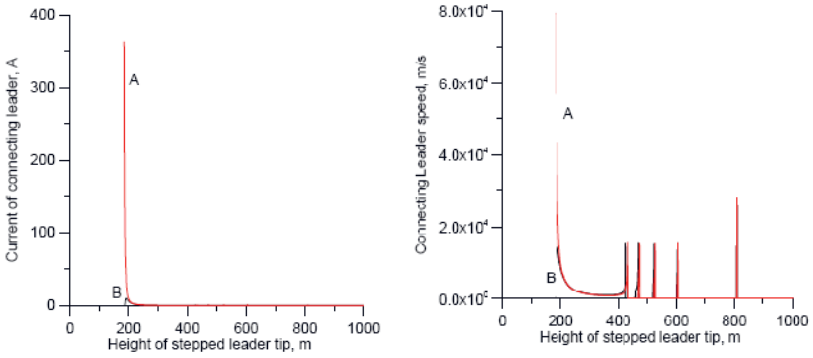

Figure 22. Current in the connecting leaders issued from rods A (red) and B (black). Taken from **Paper XIV**. Notice that the downward-coming leader is located closer to rod A than rod B (for further information, see Paper XIV).

7 Conclusions

The research work presented in this thesis has been divided into two main topics. One is numerical simulations of long gap discharges, and the other is the modelling of the lightning attachment process.

First topic "Numerical simulations of long spark gaps":

- A procedure for the calculation of long gap discharges based on physical principles was proposed. The numerical methodology was initiated with simulations of the engineering approximation of Rizk's equation for the leader channel calculation and a simplified method for the computation of the streamer zone. The methodology was improved to include a variable calculation of the streamer zone and to use the physical equations of Gallimberti to describe the potential of the leader channel. Statistical delays for the inception of the first corona and a random deviation of the path of the discharge based on experimental measurements for long spark gaps under switching impulses that were not taken into account in previous methodologies have been introduced.

- All the simulations used to validate the methodology have demonstrated that, to reproduce the discharges across long gaps under switching impulses appropriately with different electrode configurations, it is necessary to consider the streamer zone to be a variable region. Clear evidence of this can be seen in **Papers V** to **VIII**. The model has been validated and compared for different electrode configurations with successful results, and acceptable errors of less than 10% on average were obtained.

- The simulations and studies conducted have shown that, to obtain reliable values for the time to breakdown for discharges in long gaps under switching impulses, it is necessary to include the statistical delays representing the first corona inception and the random path taken by the leader channel, which depends on the electrode configuration.

- It is important to emphasize that inclusion of the statistical representation of the leader channel mainly affects the magnitude of the time to breakdown; it does not have a significant effect on the magnitude of the breakdown voltage. Preliminary simulations using the path of the discharge obtained from lightning measurements were presented in **Papers II** to **IV** and good results were obtained for the breakdown voltage. However **Papers V** to **VIII** use a random normal distribution derived from experiments conducted under switching impulses in long spark gaps in which a very good accuracy was achieved with respect to the time to breakdown. In Section 3.2.1.2 different normal distributions were calculated for the path of the discharge for a number of electrode configurations.

- The validation of the methodology is presented in Chapter 4, where recent ultra high voltage experimental tests from different electrode configurations are presented and very good accuracy in the calculation of the time to breakdown and the breakdown voltage was observed. The maximum errors obtained for the time to breakdown and the breakdown voltage were 22 and 10%, respectively.

- With the methodology developed to calculate positive discharges and the new procedure for the calculation of the streamer region, a consistent numerical simulation taking the physical process underlying the negative leader discharge into account is presented here. It includes a novel way to calculate the streamer for the pilot streamer system and enables the complete negative discharge to be predicted. The experimental results were compared with simulations and showed good agreement for the representation of the magnitudes of the current and the path taken by the discharge.

Second topic: “The lightning attachment process”

- The method applied to simulate long gap discharges described in **Papers I** to **IV** was extended to the lightning attachment simulations, and the improvements to the previous models are:
    - The space charge considered in the advance of each segment is the new charge that is generated in the region between the leader channel and the streamer zone, not only the charge that is produced in the streamer zone.
    - The background electric field takes into account the total effect of the structure. This effect was avoided in previous methodologies where linear approximations were applied.

- A calculation including the attachment of multiple upward connecting leaders from grounded structures to a downward stepped leader was introduced. It was demonstrated that the effect of one upward leader channel can reduce the electric field over the other upward leader channel incepted, thereby changing the attachment process. The results showed that a small advantage for the growth of a connecting leader from one point may drastically reduce the ability of other successful connecting leaders to be launched.

- The methodology developed was applied to test two lightning protection methods accepted in the standards: the mesh method and the cone of protection. The results have shown that the accepted methodologies are in good agreement with the physical methodology, despite the fact that they are based on engineering approximations.

8 Future Work

Two methodologies for the calculation of positive and negative long spark gap discharges under switching impulses were presented here. One of the important contributions of the methodologies was to incorporate a variable streamer region in the calculation, which had not been implemented previously in any other numerical model. The proposed methodology uses physical equations for the calculation of the development of the leader channel, and ensures that the 3D region for the streamer zone has an electric field equal to or higher than the defined streamer criteria [10]. The methodology was tested by conducting several experiments and through the use of different configurations, such as rod-rod, rod-plane, and sphere-plane configurations, and good results were obtained. Despite this good agreement, the author is of the opinion that the next step should be to apply the method to more complicated configurations, such as physical configurations presented in typical power systems, to determine its accuracy. Additionally, it would be useful for the calculation of insulation requirements in complicated configurations to analyze several spark gaps simultaneously and compare the results with experiments.

In **Papers VI** and **VIII** the methodology was applied to a rod-rod configuration. The author believes that it would be valuable to combine a self-consistent model to simulate negative leader discharges with the positive discharge, thereby representing the case when the two rods are separated a distance greater than 4m. This situation can frequently arise in ultra high voltage substations.

A preliminary model was proposed to reproduce the propagation of negative leaders, however it is the author's opinion that the negative leader process should be analyzed in greater detail, especially taking the physics behind the first pilot leader formation into account, as this has not been clearly understood by the scientific community.

The author considers that the methodology for the calculation of positive leader discharges should be extrapolated to the lightning attachment process and implemented in conjunction with the correct calculation of the streamer zone. The methodology may require a considerable amount of time to run simulations for a lightning attachment case because of the distances between

the downward-coming leader and the upward leader, however, it is still necessary to validate all the assumptions that have been made in the various models proposed.

Finally, it is the author's belief that obtaining a complete lightning attachment methodology is necessary for the downward coming leader to be modelled properly using the physics of the negative discharge. In the future, work should be dedicated to combining both negative leader discharge and positive leader discharge models.

Svensk sammanfattning

Den här avhandlingen behandlar två olika fenomen – beräkning av urladdningar vid lång stöt och långt avstånd samt uppåtgående blixtberäkning. Uppåtgående, positiva stegurladdningar och utvecklingen av urladdningar över långt avstånd består av två sammanflätade fenomen: leader - kanalen och koronaytan. Långa avståndstest från laboratorier ligger till grund för de fysiska beskrivningarna och de föreslagna beräkningarna.

Den här föreslagna metoden använder en geometrisk approximation för att representera koronaytan. Vidare används och jämförs två olika modeller för att beskriva leader-kanalen. Beräkningsmetodiken av leader-kanalen bygger på teknisk approximation kombinerat med en fysikalisk ekvation som tar med termodynamisk jämvikt. Statistik fördröjning av urladdninginges början samt en böjning av leader-kanalen infördes för att modellera ett mer realistiskt beteende hos urladdningen. En rak ledarkanal och en krokig jämfördes. Den fysiska modellen och laboratorietesterna visade god överensstämmelse.

En modell är föreslagen för att simulera negativa urladdningar vid lång stöt, med hjälp av den metod som utvecklas för att simulera positiva urladdningar och fysiken baserade på de negativa ledar fenomenen. Utvärderingen av metoden visade att fenomen som ”pilot leader” och ”negative leader current” är framgångsrikt bevisat.

En ny metod, baserad på tidigare forskning om blixtar och uppåtgående blixtar, har utvecklats och testats. Metoden förfinar tidigare beräkningar; det elektriska bakgrundsfältet och det joniserade området som beaktas för leader-segmentets progression beräknas med en alternativ metod. Den föreslagna metoden användes för att utvärdera två tekniska designmetoder som godkänts av normerna; ”the mesh method” och ”the electro geometrical method”. Resultaten visade god överensstämmelse mellan den tekniska uppskattningen och den fysiska metoden.

Det finns dock effekter av den uppåtgående blixtprocessen som inte har tagits med eller som har undvikits för att förenkla beräkningen. Faktum är att jordade konstruktioner i närvaro av ett högelektriskt fält kan producera flera uppåtgående blixter. Ändå har denna effekt inte tagits med i de olika numeriska modeller som finns tillgängliga förrän nu. De publicerade modellerna

beaktar varje uppåtgående blixt individuellt. En approximation till processen att generera flera uppåtgående blixtar presenteras här. Resultaten visar att det är möjligt att märka ett inflytande på det elektriska bakgrundsfältet när en uppåtgående blixt utvecklas samtidigt som andra uppåtgående blixtar.

Acknowledgements

First, I want to express my deepest thanks to Professor Vernon Cooray for his guidance during the years my doctoral studies have taken. I am particularly grateful to have had the opportunity and privilege to share scientific moments with a brilliant scientist. He has shown me that there is always a very easy way to look at difficult equations and concepts, and he has also shed light on my work, helping me to find solutions and clarify theories even when I thought everything was already clear! Additionally, I am very grateful for the advice that has helped me to follow a new path and look for new challenges in my life as a researcher.

I am sincerely thankful to ABB/HVDC/U Ludvika, and especially to Björn Jacobson, Dong Wu and Urban Åström. Thanks for each and every opportunity, for giving me the chance to complete my doctoral work in cooperation with industry and for being able to experience "the real work and world on the high voltage side", for all the knowledge imparted, for sharing your experience with a student, for listening to my presentations and for giving me your expert opinion and for your input to my work. Thanks to their excellent guidance, good results have been obtained in this research, which makes me feel confident to face the upcoming challenges as a researcher in the future.

No words can express my gratitude to Dr. Raul Montaño, not only for his advice, new ideas and challenges in the scientific area, but also for his help and valuable friendship.

I would like to thank all my friends and colleagues from the Lightning Research Group, Dr Mahendra Fernando, Azhlinda, Zikri, Prasan, Oscar, Mona, Dr. Prasana Liyanage, Dr. Mahbuhbur Rahman and all the others who joined our group during the time I was part of it, for their help, for the everyday learning experience about lightning or life itself, obtained during meetings or coffee breaks. I want to thank my long-time friend and trustworthy colleague Oscar Diaz especially: thanks for the time you have dedicated to understanding my work, to reviewing my writing, to debating about discharges and numerical simulations. Also, I want to express my gratitude to all my colleagues at the Division of Electricity: to the people from the "Flywheel Group" and the "Diamond Group" for the good dinners, the nice skating trips and all of the pleasant conversations in the corridors! Special thanks

to Thomas Götschl for technical help and to Gunnel Ivarsson and Ingrid Ringård for the administrative collaboration. The English structural and grammatical suggestions provided by Suzanne Lidström are deeply appreciated.

I have had the opportunity to meet many wonderful people here in Sweden, who have made me feel at home and have supported me during the good and the difficult times, in particular Marianne, Victoria, Sarah and Sra Marianne. I do not have enough words to say how grateful I am for listening, and for giving me advice and support.

There are three special people who have helped me to learn a new culture, language and way of life and I want to thank them for being so open and nice Tinus, Truls and Troy "Tack för att vara så underbara". Last, but not least, I want to express my gratitude for the support, help, patience and for all the special moments to Magnus Lindström "Tack för att göra allt så perfekt och fantastiskt till mig".

I have to express my deep gratitude to the National University of Colombia for the excellent teaching in the electrical engineering field and on high voltage technology. Furthermore, I want to thank my friends from Colombia, who always wonder how I am doing far away from home; particularly Francisco Santamaria for always been there, helping, wondering and supporting my work "Gracias pachito!"

Finally, I want to thank my family, the persons who have always stood by me, helped me and given me everything to make my dreams come true: Mujita, Mamita, Clarita, Teo, Myriamcito, Guillo, Marthica and Vivis "Alis" thanks for teaching me and giving me the most important things in my life: for teaching me to pursue my dreams, I would have never been able to achieve any of them without you. Every small step I make in my life I give thanks for having you as my family and as my support. I have no words to express how much I love all of you, thanks a lot: you are the best of my life. I want also to express my special thanks to Myriamcito, for reading my thesis, for the comments and all the effort you have put into my work.

References

1. **Group, Les Renardiéres.** Research on long air gap discharges at Les Renardieres. *Electra 23.* 1972, pp. 53–157.
2. —. Research on long air gap discharges—1973 results. *Electra 35.* 1974, pp. 47–155.
3. —. Positive discharges in long air gaps—1975 results and conclusions. *Electra 53.* 1977, pp. 31–132.
4. —. Negative discharges in long air gaps. *Electra 74.* 1981, pp. 67-216.
5. **C. Carrara, L Thione.** "Switching surge strength of large air gaps: A physical approach. *IEEE Transaction on Power Systems.* March / April 1976, Vols. Vol PAS – 95, N 2, pp. pp 512 – 524.
6. **Waters, N. I. Petrov and R. T.** Determination of the striking distance of lightning to earthed structures. *Proc. R. Soc. A 450.* 1995, pp. 589–601.
7. **Rizk, F.A.M.** Switching impulse strength of air insulation: Leader inception criterion. *IEEE Transaction on Power Delivery.* October 1989, Vol. 4, 4, pp. 2187 - 2195.
8. —. A model for switching impulse leader inception and breakdown of long air gaps. *IEEE Transaction on Power Delivery.* January 1989, Vol. 4, 1, pp. 596 - 606.
9. —. Modelling of transmission line exposure to direct lightning strokes. *IEEE Transaction on Power Delivery.* November 1990, Vol. 5, 4, pp. 1983 - 1997.
10. **Gallimberti, I.** The mechanism of long spark formation. *J. Physique Coll.* 1972, Vol. Suppl. 7 40, C7, pp. 193-250.
11. **A. Bondiou, I. Gallimberti.** Theoretical modeling of the development of the positive spark in long gaps. *Journal of Physics. D: Applied Physics.* 1994, Vol. 27, pp. 1252-1266.
12. **Lalande, P.** *"Study of the lightning stroke conditions on a grounded structure," Doctoral Thesis".* s.l. : Office National d'Etudes et de Recherches A'erospatiales (ONERA), 1996.
13. **N. Goelian, P. Lalande, A. Bondiou-Clergerie, G. L. Bacchiega, A. Gazzani, I. Gallimberti.** A simplified model for the simulation of positive-spark development in long air gaps. *Journal of Physics. D: Applied Physics.* 1997, 30, pp. 2441-2452.
14. **A. Bondio, P. Lalande, P. Laroche P, J. C. Willet, D. Davis, I. Gallimberti.** The inception phase of positive leaders in triggered light-ning: comparison of modeling with experimental data. *ICAE 99: 11th Int. Conf. on Atmospheric Electricity.* June 1999.
15. **Becerra, M and Cooray, V.** A self-consistent upward leader propagation model. *Journal of Physics. D: Applied Physics.* 2006, Vol. 39, pp. 3708–3715.
16. **Baldo G., Gallimberti I.** Breakdown phenomena of long gaps under switching impulses conditions influence of distance and voltage level. *IEEE*

Transactions on Power Apparatus and Systems. July - August 1975, Vols. PAS - 94, 4.
17. **Gallimberti I, Bacchiega G, Bondiou-Clergerie A, Lalande P.** Fundamental processes in long air gap discharges. *C.R. Physique appliquée/ Applied physics.* 2002, 3, pp. 1335 - 1359.
18. **Golde, R.** Lightning protection. *Edward Arnold.* 1973.
19. —. The lightning conductor. *Journal of the Franklin Institute.* 1967, Vol. 283, 6, pp. 451-477.
20. **Lemke, E.** "Beitrag zur abschatzung der durchschlagspannung langer luftfunkenstrecken". *Z. Elecktr. Inform u. Engietechnik.* 1973, Vol. 3, 4, pp. 186 – 192.
21. **Aleksandrov, G. N.** Special features of spark discharge development in long air clearences of insulating structures. *Elektrichestvo.* 1975, N 8, pp. pp. 15 – 18.
22. **B, Jones.** "Switching surges and air insulation". *Phil Trans R Soc. London A.* 1973, Vol. Vol 275.
23. **Hutzler.** "Leader propagation for determination of switching surge flashover voltage of large air gaps". *IEEE Transaction on Power Systems Delivery.* July/Aug 1978, Vols. Vol. PAS-97, N4, pp. pp. 1087 – 1096.
24. **Bazelyan, E.** "The leader of a long positive spark". *Electric Technology USSR.* 1987, N2, pp. pp. 47 - 60.
25. **Arevalo, Liliana.** *Numerical simulations of long spark gaps-Lightning attachment and its applications.* Uppsala : Uppsala Universitet, 2010. 0349-8352.
26. **Rizk, F.A.M.** Critical switching impulse strength of long air gaps: Modelling of air effects. *IEEE Transactions Paper Summer Power Meeting.* July/August 1991.
27. **L. Dellera, E. Garbagnati.** Lightning strike simulation by means of the leader progression model, Part I: Description of the model and evaluation of free-standing structures. *IEEE Transaction on Power Delivery.* 1990, Vols. PWRD-5, pp. 2009-2023.
28. —. Lightning strike simulation by means of the leader progression model: II. Exposure and shielding failure evaluation of overhead lines with assessment of application graphs. *IEEE Transactions on Power Delivery.* 1990, Vols. PWRD-5, pp. 2023–2029.
29. **Eriksson, A.** *The lightning ground flash –an engineering study.* Pretoria : Ph.D thesis, Faculty of Engineering, University of Natal, 1979.
30. —. An improved electrogeometric model for transmission line shielding analysis. *IEEE Transaction on Power Delivery.* July 1987, Vols. PWRD-2, N 3, pp. 871 – 886.
31. —. The incidence of lightning strikes to power lines. *IEEE Transaction on Power Delivery.* 1987, Vols. PWDR-2, pp. 859-870.
32. **D'Alessandro, F.** The use of "Field intensification factors" in calculations for lightning protection of structures. *Journal of Electrostatics.* 2003, Vol. 58, pp. 17-43.
33. **Akyuz Mose, Cooray Vernon.** The franklin lightning conductor: conditions necessary for the initiation of a connecting leader. *Journal of Electrostatics.* 2001, 51-52, pp. 319-325.
34. **D'Alessandro, N. I. Petrov and F.** Theoretical analysis of the processes involved in lightning attachment to earthed Structures. *Journal of Physics. D: Applied Physics.* 2002, Vol. 35, pp. 1788–95.

35. **A, Castellani.** *"Calcul du champ électrique par la méthode des charges equivalentes pour la simulation d'une décharge bi-leader" Doctoral thesis.* Orsay : Université Paris XI, 1995.
36. **Becerra M, Cooray V.** "A simplified physical model to determine the lightning upward connecting leader inception". *IEEE Transactions on Power Delivery.* April 2006, Vol. 21, 2, pp. 897 – 908.
37. **Becerra, M.** On the attachment of lightning flashes to grounded structures. *Doctoral Thesis.* 2008.
38. **Amarasinghe D, Sonnadara U, Berg M and Cooray V.** Channel tortuosity of long laboratory sparks. *Journal of Electrostatics.* 2007, Vol. 65, pp. 521-526.
39. **E, Idone V and Orville.** Channel tortuosity variation in Florida triggered lightning. *Geophysical Research Letters.* July 1988, Vol. 15, 7, pp. 645 - 648.
40. **L, Paris.** "Influence of air gap characteristics on line-to-ground switching surge strength". *IEEE Transaction on Power Apparatus and Systems.* August 1967, Vol. PAS 86, No. 8.
41. **Paris L, Cortina R.** "Switching and lightning impulse discharge characteristics of large air gaps and long insulator strings". *IEEE Transaction on Power Apparatus and Systems.* April 1968, Vols. PAS – 87, 4.
42. **Veldhuizen, van.** *Electrical discharges for environmental purposes: fundamentals and applications.* s.l. : New York: Nova Science, 2000. ISBN 1-56072-743-8.
43. **Yu, Dyakonov M I and Kachorovskii V.** Zh. Eksp. Teor. Fiz. *Soviet Physics JETP.* 1988, Vol. 67, 1049.
44. **ABB PS/HVDC Ludvika.** *Switching impulse tests for different electrode gap configurations.* Ludvika : s.n., 2006.
45. **Ming Li, Wu Dong, Åström Urban and Asplund Gunnar.** Intriguing observation on the breakdown trajectory of large air-gaps under switching impulse voltages. *16th International symposium on high voltage engineering.* 2009.
46. **ABB PS/HVDC R&D.** *Experimental investigations of air insulation.* Ludvika : ABB, 2010.
47. **Commission, IEC International Electrotechnical.** *IEC 60060-1 High voltage test techniques - Part 1 General definitions and test requirements.* s.l. : IEC, 2010. ISBN 978-2-88912-185-4.
48. **ABB PS/HVDC Ludvika Wu Dong, Ming Li, Åström U, Ericsson A.** *Experimental investigation of air insulation under positive switching impulse voltage for HVDC System (Part 1. Sphere/plane air gaps). ABB Internal confidential report.* Ludvika : s.n., 2006.
49. **Castellani A., Bondiou A, Lalande P, Bonamy A and Gallimberti I.** Laboratory study of the bi-leader process from an electrically floating conductor Part 2: Bi-leader properties. *IEE Proc. Sci Meas Technol.* September 1998, Vol. 145, 5.
50. **Lalande P., Bondiou-Clergerie A, Bacchiega G., Gallimberti I.** Observations and modeling of lightning leaders. *C.R. Physique.* 2002, Vol. 3, pp. 1375-1392.
51. **Dellera L, Garbagnati E.** Lightning stroke simulation by means of the leader progression model Part I: Description of the model and evaluation of free-standing structures. *IEEE Transaction on Power Delivery.* 1990, Vols. PWRD-5, Issue 4, pp. 2009-22.
52. **Bacchiega G, Gazzani A, Bernardi M, Gallimberti I, Bondiou A.** Theoretical modelling of the laboratory negative stepped leader. *Proceedings of the 1994*

international Aerospace and Ground conference on Lightning and Static Electricity. 1994.
53. **Mazur V, Ruhnke L, Boundiou-Clergerie and Lalande P.** Computer simulation of a downward negative stepped leader and its interaction with ground structures. *Journal of Geophysical Research.* September 2000, Vol. Vol 105, No. D17, pp. page 361 – 369.
54. **Niemeyer L, Pictronero L, Wiesmann H.** Fractal dimension of dielectric breakdown. *Phys. Rev. Lett.* 1984, 52, pp. 1033-1036.
55. **J, Tsonis A and Eisner.** Fractal characterization and simulation of lightning. *Beitr. Phys Atmos.* 1987, Vol. 60, (2), pp. 187-192.
56. **Sanudo J, Gomez J, Castaño F and Pacheco A.** Fractal dimensions of lightning discharge. *Non-linear Process in Geophysics.* 1995, Vol. 2, pp. 101 - 106.
57. **G, Petrova.** Lightning stroke simulation by means of the fractal approach: Attractive and protective zones for structures. *24th International Conference on Lightning Protection.* 1999.
58. **Beroual A, Rakotonandrasana J, Fofana I.** Predictive dynamic model of the negative lightning discharge based on similarity with long laboratory sparks – part 1: physical process and modeling. *IEEE Transactions on Dielectrics and Electrical Insulation.* October 2010, Vol. 17, 5, pp. 1551 – 1561.
59. —. Predictive dynamic model of the negative lightning discharge based on similarity with long laboratory sparks – part 2: Validation. *IEEE Transactions on Dielectrics and Electrical Insulation Vol 17, N 5, 1562 – 1568.* 2010.
60. **Arevalo L, Cooray V and Montano R.** Numerical simulation of long laboratory sparks generated by positive switching Impulses. *Journal of Electrostatics.* May 2009, Vol. Vol 67, Issue 2 – 3.
61. **Arevalo L, Cooray V and Wu D.** Laboratory long gaps simulation considering a variable corona region. *International Conference on Lightning Protection. ICLP – 2010.* 2010.
62. **IEC.** International standards on protection against lightning Part 1. General principles. IEC 62305 -1. Geneva, Switzerland : s.n., 2006.
63. —. International standards on protection against lightning Part 2. Physical damage to structures and life hazards. IEC 62305 -3. Geneva, Switzerland : s.n., 2006.
64. **H. R. Armstrong, E. R. Whitehead.** A lightning stroke pathfinder. *IEEE Trans. Power Apparatus and systems.* 1964, Vol. 83, pp. 1223-1227.
65. —. Field and analytical studies of transmission line shielding. *IEEE Trans. Power Apparatus and systems.* 1968, Vol. 87, pp. 270-279.
66. **G. W. Brown, E. R. Whitehead.** Field and analytical studies of transmission line shielding: Part II. *IEEE. Trans. Power Apparatus and Systems.* 1969, Vol. 88, 5, pp. 617-625.
67. **D. W. Gilman, E. R. Whitehead.** The mechanism of lightning flashover on high voltage and extra-high voltage transmission lines. *Electra.* 1973, Vol. 27, pp. 65-96.
68. **C. F. Wagner, G. D. McCann, G. D. and G. L. MacLane.** Shielding of transmission lines. *AIEE Transactions.* 1941, Vol. 60, pp. 313-328.
69. **C. F. Wagner, G. D. McCann, C. M. Lear.** Shielding of substations. *AIEE Transactions.* 1942, Vol. 61, pp. 96-100.
70. **Golde, R.** The frequency of occurrence and the distribution of lightning flashes to transmission lines. *Transactions AIEE.* 1945, Vol. 64, pp. 902 - 910.

71. **Wagner C, Hileman R.** “The lightning strike” II. *Trans. AIEE.* 1961, Vol. 80, pp. 622 – 642.
72. **Young, Clayton, Hileman.** Shielding of transmission lines. *IEEE Transaction on Power and Apparatus and Systems (supplement).* 1963, Vol. 83, pp. 132 - 154.
73. **Flisowski, Z.** Trends in the lightning protection of structures. *PWN.* 1986.
74. **Horvarth, T.** *Computation of lightning protection electronic and electrical engineering research studies.* New York : Series Wiley, 1991.
75. **IEEE, The Institute of Electrical and Electronics Engineers.** *Std 998-1996, IEEE Guide for direct lightning stroke shielding of substations.* 1996. ISBN 1-55937-768-2.
76. **Becerra, M, Cooray, V and Hartono, A.** Identification of the lightning vulnerable points on complex grounded structures. *Journal of Electrostatics.* 2007.
77. **Becerra M, Cooray V, Roman F.** Lightning striking distance of complex structures. *IET Generation Transmission and Distribution.* 2008, Vol. 2, pp. 131 - 138.
78. **Cooray V., Rakov V., Theethayi N.** The lightning striking distance - Revisited. *Journal of Electrostatics.* 2007, Vol. 65, pp. 296 – 306.
79. **EPRI.** *Transmission line reference book 345kV and above.* s.l. : EPRI, 1982. 2nd edition.

Acta Universitatis Upsaliensis

Digital Comprehensive Summaries of Uppsala Dissertations from the Faculty of Science and Technology 820

Editor: The Dean of the Faculty of Science and Technology

A doctoral dissertation from the Faculty of Science and Technology, Uppsala University, is usually a summary of a number of papers. A few copies of the complete dissertation are kept at major Swedish research libraries, while the summary alone is distributed internationally through the series Digital Comprehensive Summaries of Uppsala Dissertations from the Faculty of Science and Technology. (Prior to January, 2005, the series was published under the title "Comprehensive Summaries of Uppsala Dissertations from the Faculty of Science and Technology".)

Distribution: publications.uu.se
urn:nbn:se:uu:diva-149171

ACTA
UNIVERSITATIS
UPSALIENSIS
UPPSALA
2011